Master's thesis

NTNU
Norwegian University of Science and Technology
Faculty of Information Technology and Electrical Engineering
Department of Electric Power Engineering

Sivert Forbord
Håkon Sølberg

Integration of Power Transfer Distribution Factors and Internal Grid Constraints in Short-Term Hydropower Scheduling

Master's thesis in Energy and Environmental Engineering
Supervisor: Olav B. Fosso
Co-supervisor: Per Aaslid, Hans Ivar Skjelbred
June 2023

NTNU
Norwegian University of
Science and Technology

Sivert Forbord
Håkon Sølberg

Integration of Power Transfer Distribution Factors and Internal Grid Constraints in Short-Term Hydropower Scheduling

Master's thesis in Energy and Environmental Engineering
Supervisor: Olav B. Fosso
Co-supervisor: Per Aaslid, Hans Ivar Skjelbred
June 2023

Norwegian University of Science and Technology
Faculty of Information Technology and Electrical Engineering
Department of Electric Power Engineering

NTNU
Norwegian University of
Science and Technology

Abstract

With the growing electricity demand, maximizing the utilization of our resources and infrastructure becomes crucial. In countries like Norway, this entails effectively utilizing the transmission grid and harnessing the potential of water stored in hydropower reservoirs. In *Short-Term Hydro Scheduling* (STHS), grid limitations are often not included in the optimization process. This thesis aims to explore the implementation of *Power Transfer Distribution Factors* (PTDF) in the STHS problem to enable grid-constrained optimization.

To highlight the applications of PTDF, a series of optimizations were run in the STHS tool SHOP, developed by SINTEF ER. A system model replicating the Norwegian price zone NO4 was developed for the optimizations, and a standalone Python module was designed to generate the PTDF factors. The optimization results showcase the diverse applications of PTDF. These encompass power flow calculation, enforcing flow restrictions, the utilization in contingency analysis and congestion management, and its effectiveness in calculating power flows within specific sub-zones of the system.

Insights derived from the case studies were employed to explore different levels of PTDF implementation in the electricity market clearing process. The discussion encompassed various pricing approaches, including nodal pricing and zonal pricing with FBMC. Including grid constraints in the market clearing algorithm introduces complexities related to market manipulation and unfair market positions. Enhanced collaboration between Transmission System Operators and power producers is needed to address these challenges. The discussion on the PTDF module recognized the benefits of having a dedicated module capable of generating constraints for the optimization problem. Apart from generating PTDF, the module was also assessed for its potential to incorporate contingency analysis and congestion management techniques.

In conclusion, utilizing *Power Transfer Distribution Factors* in STHS and in the market clearing shows great promise. However, unlocking its full potential relies on establishing a robust system to ensure a just and equitable power market.

Sammendrag

Med økende forbruk av elektrisk energi blir det avgjørende å maksimere utnyttelsen av våre ressurser og infrastruktur. I et land som Norge innebærer dette effektiv bruk av strømnettet og utnyttelse av vannet som er lagret i vannkraftreservoarer. Korttids-vannkraftplanlegging (STHS) tar vanligvis ikke hensyn til begrensninger i strømnettet i optimaliseringsprosessen. Denne avhandlingen har som mål å utforske implementeringen av *Power Transfer Distribution Factors* (PTDF) i vannkraftplanlegging for å muliggjøre optimalisering med hensyn til nettbegrensninger.

For å belyse bruksområdene til PTDF ble det gjennomført en serie optimaliseringer i STHS-verktøyet SHOP, utviklet av SINTEF ER. En systemmodell som gjenskaper den norske prissonen NO4 ble satt sammen, og en frittstående Python-modul ble utviklet for å generere PTDF-faktorene. Resultatene viser forskjellige bruksområder for PTDF, blant annet beregning av kraftflyt, håndheving av kraftflytbegrensninger, bruk i utfallsanalyse og håndtering av flaskehalser.

Lærdom fra optimaliseringene ble brukt til å utforske ulike nivåer av PTDF-implementering i markedsklareringen. Diskusjonen omfattet ulike tilnærminger, inkludert nodeprising og soneprising med FBMC. Inkluderingen av nettbegrensninger i markedsklareringen introduserer problemstillinger knyttet til markedsmakt. Det er behov for økt samarbeid mellom nettselskaper og kraftprodusenter for å håndtere disse utfordringene. Diskusjonen om PTDF-modulen anerkjente fordelene med å ha en dedikert modul som er i stand til å generere begrensninger for optimaliseringsproblemet. Potensialet for å inkludere utfallsanalyse og håndtering av flaskehalser i modulen er verdt å nevne.

Konklusjonen er at bruk av *Power Transfer Distribution Factors* i korttids-vannkraftplanlegging og i markedsklareringen har stort potensiale. Dette potensialet er dog avhenging av at det etableres et system for å sikre et rettferdig kraftmarked.

Preface

This master's thesis was completed during the spring of 2023 at the Department of Electric Energy at the Norwegian University of Science and Technology (NTNU). The task was initiated by SINTEF Energy Research to investigate power flow functionality in their hydro scheduling tool SHOP, a subject that fascinated us both. With the fortune of securing our preferred specialization project in the autumn of 2022, we embarked on this exciting task together. As our collaboration continued, it naturally evolved into the subject of our master's thesis.

We want to express our heartfelt gratitude to our head supervisor, Professor Olav B. Fosso, at NTNU. His dedication to the topic and insightful feedback has greatly contributed to the quality of this thesis. We would also like to extend our sincere appreciation to our co-supervisors, Hans Ivar Skjelbred and Per Aaslid from SINTEF Energy Research. In particular, we are deeply grateful to Per Aaslid for his continuous availability and assistance in resolving numerous problems that arose during the course of our work.

Finally, as we conclude this thesis, we eagerly anticipate embarking on our professional journey and applying the knowledge and skills gained throughout our research. As we transition into this new phase of our lives, we cherish the invaluable friendships that have formed over these five years of study. Thank you all!

Trondheim, 08/06/2023

Håkon Sølberg

Sivert Forbord

Contents

List of abbreviations

ATC	Available Transmission Capacity
CB	Critical Branches
CNTC	Coordinated Net Transmission Capacity
DCPF	DC Power Flow
FBMC	Flow-based Market Coupling
FCR	Frequency Containment Reserves
FERC	Federal Energy Regulatory Commission
GSK	Generation Shift Keys
HPF	Hydropower Production Function
IEA	International Energy Agency
I/O	Input/Output
LODF	Line Outage Distribution Factor
LP	Linear Programming
MCP	Market Clearing Price
MILP	Mixed-Integer Linear Programming
NVE	Norwegian Water Resources and Energy Directorate
OPF	Optimal Power Flow
PTDF*	Power Transfer Distribution Factor
RAM	Remaining Available Margin
REM	Energy Regulatory Authority
SHOP	Short-term Hydropower Optimization Program (software).
STHS	Short-term Hydro Scheduling
TSO	Transmission System Operator
UC	Unit Commitment mode
ULD	Unit Load Dispatch mode
X/R	Reactance/resistance

∗ The PTDF abbreviation is mainly used for PTDF as a concept, while "PTDF factors" is often used when referencing the individual distribution factors.

Nomenclature

Parameters

a_{ij}	Power transfer distribution factor of branch.
$C_{i,s}$	Start-up cost of unit i in plant s (NOK).
$C_{i,s}^{PEN}$	General cost penalty parameter (NOK).
E_S	Energy conversion factor for plant s ($\frac{MWh}{m^3}$).
F_{ij}	Maximum active flow on line from node i to j (MW).
M_t^{BUY}	Market price of bought energy in period t ($\frac{NOK}{MWh}$).
M_t^{SELL}	Market price of energy in period t ($\frac{NOK}{MWh}$).
$P_{i,s}^{MIN}, P_{i,s}^{MAX}$	Minimum and maximum production of unit i in plant s (MW).
$Q_{k,t}^{NI}$	Forecasted natural inflow into reservoir k in period t ($\frac{m^3}{s}$).
Q_S^{MIN}, Q_S^{MAX}	Minimum and maximum discharge of plant s ($\frac{m^3}{s}$).
V_k^{MIN}, V_k^{MAX}	Minimum and maximum water volume of reservoir k (m^3).
$W_{k,t}^{END}$	Water value of reservoir k at the end of scheduling horizon t ($\frac{NOK}{MWh}$).
G	Conversion constant including the gravity acceleration, $9.81{\cdot}10^{-3}$ ($kg \cdot \frac{m^2}{s^2}$).

Sets and indexes

B	Set of buses, index $\in B$.
I_S	Set of hydro-turbine generator units in plant s, index $\in I_S$.
K	Set of reservoirs, index k $\in K$.
L	Set of lines, index $\in L$.
S	Set of hydropower plants, index s $\in S$.
T	Set of time periods, index $\in T$.

Variables and state-dependent functions

β	General penalty function variable.
$\eta_{i,s}^{GEN}$	Generator efficiency of unit i in plant s as function of production of the unit (%).
$\eta_{i,s}^{TURB}$	Turbine efficiency of unit i in plant s as a function of net head and water discharge (%).
$\mu_{i,s,t} \in \{0,1\}$	Start-up decision of unit i in plant s in period t (1 if it is started up in period t, 0 otherwise).
$\omega_{i,s,t} \in \{0,1\}$	Status of unit i in plant s in period t (1 on, 0 off).

$h_{i,s,t}^{NET}$	Net head of unit i in plant s in period t (m).
$p_{i,s,t}$	Power output of unit i in plant s in period t ($\frac{m^3}{s}$).
$q_{i,s,t}$	Water discharge of unit i in plant s in period t ($\frac{m^3}{s}$).
$Q_{i,s,t}^{MAX}(h_{i,s,t}^{NET})$	Maximum water discharge of unit i in plant s in period t as a function of the net head ($\frac{m^3}{s}$).
$Q_{i,s,t}^{MIN}(h_{i,s,t}^{NET})$	Minimum water discharge of unit i in plant s in period t as a function of the net head ($\frac{m^3}{s}$).
$q_{k,t}^{BYPASS}$	Water released via bypass gate of reservoir k in period t ($\frac{m^3}{s}$).
$q_{k,t}^{TOTAL}$	Total regulated water release of reservoir k in period t ($\frac{m^3}{s}$).
$v_{k,t}$	Water volume of reservoir k at the end of period t (m^3).
p_t^{SELL}	Power sold to the market in period t (MW).

Some of the same notations can be found in Ref. [1].

List of Figures

List of Tables

1 Introduction

Hydropower scheduling, transmission utilization, and restructuring of energy systems will be essential to reach the goal of a reliable grid towards 2040. The introduction provides an overview of the background of the master's thesis, current articles related to the topic, and the problem approach.

1.1 Project Background

According to Statnett, Norwegian electricity consumption could grow from 140 TWh in 2021 to 220 TWh in 2050. The demand for renewable energy is increasing, and more power-demanding industries want to connect to the grid. Statnett's short-term market analysis indicates that Norway could experience an electricity deficit already in the mid-2020s. A significant part of the expected consumption growth is power-intensive industries like data centers and the production of batteries and hydrogen [2, 3].

In the first half-year of 2022, the difficult situation in the European energy markets pushed power prices to a historical high. The situation in the power markets and restrictions in transmission capacity has resulted in high price differences between southern Norway and central and northern parts of Norway. Low reservoir levels in southern Norwegian reservoirs, combined with the shortage of gas in Europe because of the war in Ukraine, have increased the uncertainty related to the security of supply. Halfway into 2022, overall reservoir levels in Norway were at 59.2 % of capacity, 8.7% below normal. In southern Norway, reservoir levels were significantly lower, and down to 45.5 % of capacity in price zone NO2 [4].

Restructuring energy systems, industrial investments, and higher shares of intermittent power will require the best possible utilization of the existing power grid. Statnett is working on several measures to increase the grid performance. An example is the joint Nordic project to optimize the calculation of available capacity. This method is known as *Flow-Based Market Coupling* (FBMC) [4]. The physical characteristics and limitations of the power grid are entered directly into the market algorithm. The grid capacity is distributed and prioritized as part of market optimization and will ensure better utilization of the Norwegian power grid [5]. By leveraging FBMC and similar approaches, the

Norwegian power grid will be utilized more efficiently, ensuring reliable and sustainable power transmission for the evolving energy landscape.

1.2 Problem Statement and Approach

The objective of this thesis is to examine the effects of incorporating internal grid limitations into *Short-Term Hydropower Scheduling* (STHS). This is accomplished by integrating *Power Transfer Distribution Factors* (PTDF) into the STHS tool SHOP (Short-term Hydro Optimization Program). A 14-bus system located within the Norwegian price zone NO4 is modeled and simulated. The findings and insights obtained from these simulations are then utilized to analyze the influence of various levels of PTDF implementation in STHS and its broader implications for the electricity market.

The main questions to be addressed in this report is:

- How can grid limitations be taken into account for *Short-Term Hydro Scheduling*?
- How will the optimal operation of hydropower plants be affected by taking grid limitations into account?
- How can *Power Transfer Distribution Factors* be utilized in STHS?
- How can *Power Transfer Distribution Factors* be utilized in the electricity market?

1.3 Contribution

This master's thesis contributes to the field of power system optimization and analysis, specifically in the context of hydro scheduling within the SHOP framework. The key contributions of this study can be summarized as follows:

- Developed a standalone Python module for calculation of PTDF factors.
- Exemplified and discussed the applications of PTDF in the SHOP environment. Developed an extensive model of Norwegian price zone NO4 within the SHOP framework, and ran several optimization scenarios.
- Highlighted opportunities and provided suggestions for further use of PTDF in SHOP, including congestion management and contingency analysis.

- Provided insightful reflections on how PTDF can be implemented into the general electricity market clearing algorithm, and the impact it may have.

1.4 Literature Review

This literature review explores various studies that investigate the incorporation of network constraints and power flow equations in the context of hydro scheduling. The findings from the reviewed studies include improved decision-making, improved system utilization, and enhanced economic and operational performance.

In Ref. [6], the network constraints were included in the *Short-term Hydro Scheduling* (STHS) problem due to the number of hydro plants located far from the load. Hydroelectric and thermal plants are coordinated to supply the demand at a minimum cost based on a set of constraints. The method proposed is based on Lagrangian Relaxation (LR) with data from the Brazilian Hydrothermal power system. The results show that, for a power system with hydropower plants located far from the load, the system needs a detailed modeling for the transmission system.

In Ref. [7], the influence of including power flow equations in the STHS problem was investigated. The study examined three different case studies for the northernmost price zone in Norway, NO4. First, a base case is constructed to simulate how STHS is conducted today. The system topology and restrictions for production planning were neglected, and the result was used as a reference point. The two other cases considered other known bottlenecks in the transmission system in Finnmark. The result showed that less economic decisions had to be made when accounting for the power grid.

Ref. [8] studied the effect of coordinating hydro and wind power production in a transmission-constrained region. The transmission lines are modeled as constraints on the amount of power that can be exchanged with the external market. The internal transmission constraints are not included in Ref. [8], but Ref. [9] used *Power Transfer Distribution Factors* (PTDFs) for modeling the flow constraints. The model was tested on data from the Icelandic power system, with a simulation period of 169 weeks. Modeling the limited transmission capacity between the major watercourses significantly impacted

the estimated balancing potential on Iceland. Simulations without power flow constraints overestimated the capability of exporting power to the UK market and gave unrealistic reservoir operations.

In Ref. [10], two different approaches of considering capacity calculation were compared in the Nordic region. The current method of Coordinated Net Transmission Capacity (CNTC) and FBMC was analyzed. The results indicated that total welfare increases and differences between average prices are smaller when using FBMC instead of CNTC, especially on a power system with increased wind power capacity. Since the FBMC model handles bottlenecks more effectively than the CNTC model, it can use more wind and run-of-river energy.

The study described in Ref. [11] focused on an area in Northern Norway with limited grid capacity, high wind potential, and existing hydropower. The simulations aimed to investigate the impact of the grid regulations (NEM) introduced in Norway in 2019, specifically on the optimal utilization of transmission capacity in an energy loss minimization model. The results showed that a large portion of the transfer capacity was left unused throughout the simulated year, with an annual capacity surplus of 45.76%.

Table 1.1: *Literature review*

Title and reference	Author	Country/area	STHS?	Objective
Solving the hydrothermal scheduling problem considering network constraints. (2012) [6]	Fabricio Takigawa et.al	Brazil	Yes	Minimize total operation cost
The Influence on Day-Ahead Trading Volumes by Including Power Flow Equations in The Planning Algorithm for Short-Term Hydropower in Congested Areas. (2022) [7]	Marius Eriksen & Mathias Trondal	Northern Norway	Yes	Minimize value of water used to cover load obligation.
Coordination of hydro and wind power in a transmission constrained area using SDDP. (2016) [8]	Espen F. Bødal et.al	Western Norway	LTHS	Maximize energy sales
A model for optimal scheduling of hydro-thermal systems including pumped-storage and wind power. (2013) [12]	Arild Helseth et.al	Iceland	MTHS and LTHS	Maximize energy sales
The impact of Flow-Based Market Coupling on the Nordic region (2020) [10]	Andreas H. Bø et.al	Nordic region	No	Minimize production cost
Optimal Utilisation of Grid Capacity for Connection of New Renewable Power Plants in Norway. (2021) [11]	Viljar S. Stave et.al	Northern Norway	HS	Energy loss minimization

MTHS Medium-term hydro scheduling
LTHS Long-term hydro scheduling

1.5 Outline

Introduction - Provides an introduction to the thesis, including the underlying motivation and problem statement. Summarizes the significant contributions made throughout the thesis.

Theory - Contains relevant theory about *Short-Term Hydro Scheduling* and the Nordic Electricity Market. Introduces *Power Transfer Distribution Factors* and discusses their relevance. Provides an overview of the STHS tool SHOP, developed by SINTEF ER, and its significance in the research.

Methodology - Describes the system model and different cases used in the SHOP simulation. Offers a comprehensive explanation of the SHOP optimization problem and outlines the process of acquiring data for the simulations. Describes the development of the PTDF module specifically designed for generating PTDF factors for the SHOP model.

Results - Presents the most significant and relevant outcomes derived from the various case studies conducted. Emphasizes key aspects and provides a comparative analysis.

Discussion - Analyzes and interprets the results obtained from the case studies, addressing their implications in relation to the problem statement. Explores potential applications and future prospects of the PTDF module, along with reflection on how the electricity market can benefit from PTDF utilization. Contains a critical evaluation of the data employed in the system model.

Conclusion - Summarizes the main findings and their implications with respect to the problem statement. Provides a concise overview of the research outcomes.

Appendix - Includes detailed examples illustrating the construction of data for inflow, water value, and line information. Contains supplementary results from the simulations, along with examples of SHOP input data.

Disclaimer: The theoretical concepts discussed in Section 2.1 and 2.3 of this thesis draw heavily from our specialization project[13] and may exhibit similarities in content and structure.

2 Theory

This chapter introduces important topics related to *Short-Term Hydro Scheduling* (STHS), transmission modeling and *Power Transfer Distribution Factors* (PTDF). Furthermore, it provides a theoretical description of the STHS optimization problem, along with the most significant constraints.

2.1 Hydropower Scheduling

The hydropower scheduling problem is commonly decomposed into long-term, medium-term, and a short-term problem. Each of these problems is solved by dedicated models and solutions techniques [14]. At its core, the purpose of hydropower scheduling is to determine where and when to generate hydroelectric power. By leveraging the combination of these three solution techniques, a practical and optimal solution to this question can be achieved. In general, uncertainties are modeled in detail in the long and medium-term problems, and the system constraints are precisely detailed in the short-term problem [6]. The toolchain illustrated in Figure 2.1 shows each of the key tools developed by SINTEF Energy Research (ER) for different scheduling purposes, marked in red [12].

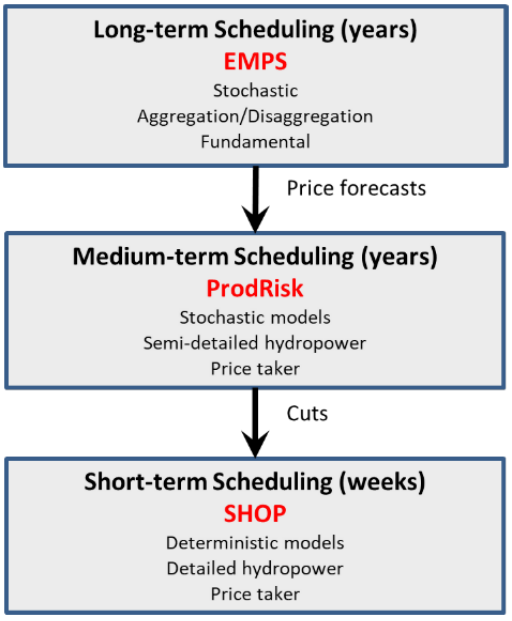

Figure 2.1: *Key models developed by SINTEF Energy Research for different scheduling purposes [12].*

The long-term models estimate strategies for using the water in the entire planning pe-

riod. These are stochastic models where uncertainties in inflows and market prices are presented. The medium-term model may be seen as a link between the long and short-term scheduling models. The medium-term model typically has a planning horizon of one year and a time increment of one week. The models used for STHS serve to further define the level of technical detail for a short time period in a deterministic way [15]. The level of detail in these models is of utmost importance, as it directly influences the decision-making process regarding the actual physical operation of hydropower plants.

2.1.1 Optimization problems

Since the approach to solving hydropower scheduling involves optimization problems, providing a concise description of these types of problems could be useful. An optimization problem can be described as trying to find the best solution while satisfying a set of restrictions or criteria [16]. An optimization problem consists of three main components:

1. *The objective function*, which is the problem you are trying to find the optimal solution to.
2. *Decision variables*, which are the unknown variables in the objective function, whose final values will be the solution to the optimization problem.
3. *Constraints*, which are equations that limit the feasible solution range of the objective function.

By combining these components the optimization problem can be expressed mathematically:

$$\begin{aligned} &\text{min/max:} && h_0(\mathbf{x}) && \\ &\text{subject to:} && f_i(\mathbf{x}) \leq 0 && i = 1, ..., m \\ &&& h_j(\mathbf{x}) = 0 && j = 1, ..., p \end{aligned} \tag{2.1}$$

, where h_0 is the objective function, $\mathbf{x}$ is a list of decision variables, and f_i and h_i are constraint equations. Depending on the nature of the objective function, the optimal solution for such optimization problems can be found through linear programming.

2.1.2 The STHS optimization problem

The STHS problem focuses on searching for the most economical schedules among the generating units to meet the load demand while satisfying the system constraints. In a deregulated power system like the Norwegian, each hydro producer maximizes their profits by trading electricity in a competitive electricity market. The assumption is that the power producers do not have the market power to influence the market price. In STHS, the objective function could be expressed as the following: [1, 17]

$$\text{Max} \sum_{t \in T} M_t^{SELL} \cdot \Delta T \cdot p_t^{SELL} + \sum_{k \in K} W_{k,t}^{END} \cdot E_S \cdot v_{k,t} - \sum_{t \in T} \sum_{s \in S} \sum_{i \in I_S} C_{i,s} \cdot \mu_{i,s,t} \qquad (2.2)$$

where

M_t^{SELL}	Forecasted market price of electricity in period t.
Δ T	Length of each period (hour).
p_t^{SELL}	Power sold to the market in period t (MW).
$W_{k,t}^{END}$	Marginal water value of reservoir k at the end of the scheduling horizon t ($\frac{NOK}{MWh}$).
E_S	Energy conversion factor for plant s ($\frac{MWh}{m^3}$).
$v_{k,t}$	Water volume of reservoir k at the end of period t (m^3).
$C_{i,s}$	Start-up cost of unit i in plant s (NOK).
$\mu_{i,s,t}$	Start-up decision of unit i in plant s in period t (1 or 0).

The optimization problem is a trade-off between using water now and saving it for future power production. The first term in Equation (2.2) refers to the total profit from selling energy in the current market. The second term is the future income by storing water at the end of the optimization period. The last term is the start-up cost of each unit. As the start-up and shut-down costs significantly impact the STHS, each unit's start-up cost should be minimized [1, 17].

2.1.3 Hydropower Production

The hydropower production function (HPF) is determined by water discharge through the unit and the net head of the connected reservoir. Equation (2.3) is a non-linear and non-convex function, also known as the hydro unit generating input/output (I/O) characteristic [1].

$$p_{i,s,t} = G \cdot \eta_{i,s}^{GEN}(p_{i,s,t}) \cdot \eta_{i,s}^{TURB}(h_{i,s,t}^{NET}, q_{i,s,t}) \cdot h_{i,s,t}^{NET} \cdot q_{i,s,t} \tag{2.3}$$

where

$p_{i,s,t}$	Power output of unit i in plant s in period t (MW).
G	Conversion constant ($9.81 \cdot 10^{-3}$ kg $\frac{m^2}{s^2}$).
$\eta_{i,s}^{GEN}(p_{i,s,t})$	Generator efficiency of unit i in plant s as a function of the production of the unit (%).
$\eta_{i,s}^{TURB}(h_{i,s,t}^{NET}, q_{i,s,t})$	Turbine efficiency of unit i in plant s as a function of the net head and water discharge of the unit (%).
$h_{i,s,t}^{NET}$	Net head of plant s in period t (m).
$q_{i,s,t}$	Water discharge of unit i in plant s in period t ($\frac{m^3}{s}$).

The generator and turbine efficiency have a significant impact on the power output. For a given net head, the turbine efficiency can be as low as 60% at minimum discharge and as high as 95% at the best efficiency point. Considering the trade-off between accurately representing the HPF and computational efficiency is important. The turbine efficiency could be expressed as a fixed value or flow-dependent [1].

2.1.4 Power balance and water release

The outflow consists of regulated and unregulated water release. As expressed in Equation (2.4), the regulated release refers to the total discharge of the units, while the unregulated refers to the flow through bypass gates. This flow can be regulated to balance the minimum outflow constraints and the transmission capacity limits [1]. In a competitive market like the Norwegian system, the power can be sold to the market. This relationship is represented by the energy balance constraint for the plant in Equation (2.5).

$$q_{k,t}^{TOTAL} = \sum_{i \in I_S} q_{i,s,t} + q_{k,t}^{BYPASS} \tag{2.4}$$

$$\sum_{s \in S} \sum_{i \in I_S} p_{i,s,t} = p_t^{SELL} \tag{2.5}$$

where

$q_{k,t}^{TOTAL}$	Total regulated water release of reservoir k in period t ($\frac{m^3}{s}$).
$q_{i,s,t}$	Water discharge of unit i in plant s in period t ($\frac{m^3}{s}$).
$q_{k,t}^{BYPASS}$	Water released via bypass gate of reservoir k in period t ($\frac{m^3}{s}$).

$p_{i,s,t}$ Power output of unit i in plant s in period t (MW).

p_t^{SELL} Power sold to the market in period t (MW).

Optimization problem structure

Figure 2.2 shows a conceptual representation of the STHS optimization problem, where the blue blocks represent optimization constraints and to which time intervals they are coupled. The blue color that bleeds out from the diagonal elements symbolizes how the optimization variables for a time interval can impact the constraints of other time intervals. An example of such a variable is *reservoir content*. The state of the reservoir in the preceding interval will affect the discharge calculation of the present interval, which, in turn, will affect the calculation of the subsequent interval.

In addition, the optimization process is subject to boundary constraints due to its coupling with medium-term scheduling. This coupling is denoted by the *(T=N+)* row/column. Due to the time interval coupling and boundary conditions, the STHS problem assumes a network-like structure, illustrated in Figure 2.2. The blue bar at the bottom of the figure represents constraints that are active for all time intervals. The PTDF grid limitation constraints discussed in this paper belong to this category. [13, 18].

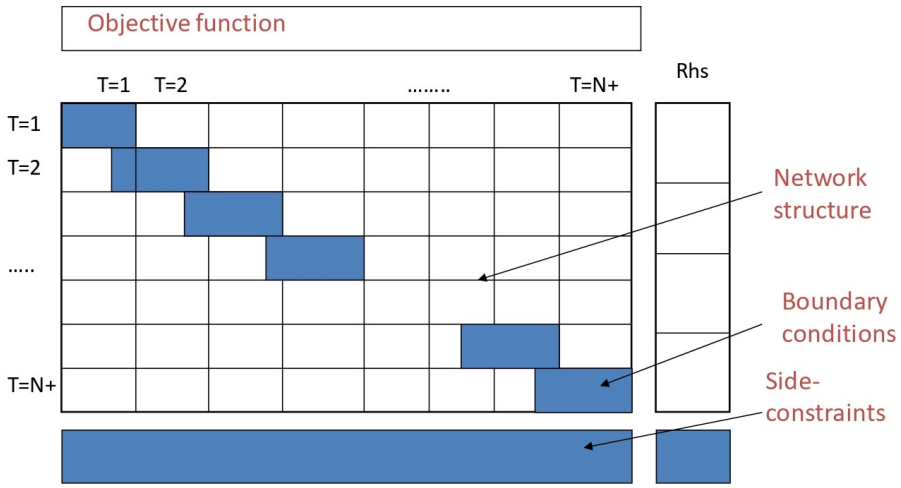

Figure 2.2: *Conceptual structure of the STHS optimization[18].*

2.1.5 Water values

To manage a hydropower facility successfully, producers must be able to accurately calculate whether the marginal value of their stored water is greater than market prices at any given time. If this proves factual, they can withhold power production until pricing conditions are favorable. This core principle of hydropower scheduling highlights the importance of correctly estimating the marginal value of water stored in a reservoir. The marginal value of water stored in a reservoir is commonly referred to as *water value*.

Multiple factors influence the water value of a reservoir. The most critical factors are reservoir levels, overall plant input/output efficiencies (which determine how efficiently water gets converted into electricity), water inflow, operational costs, and accurate pricing expectations over both short- and long-term periods. The last factor is particularly important, as the difference between market price and water value is the deciding factor between choosing to produce or not. This factor is again influenced by the availability of other energy sources, like fossil fuels and renewable power. As the market price reflects the relationship between power demand and power production, the composition of available power production is of great significance [19].

Due to the wide range of factors influencing the water value, and especially the stochastic nature of e.g. inflow and power market forecasts, the calculation of water values can be strenuous and complex. Therefore, most solution strategies include advanced models and stochastic linear programming. One of the aspects that complicate the calculation is cascaded water courses. The utilization and evaluation of water in one reservoir will affect and is dependent on the water values of affiliated reservoirs. However, as stated in Ref. [20], having dependent water values is the preferred theoretical solution. Overall, the process of calculating water values for hydropower scheduling involves a combination of data analysis, mathematical modeling, and careful management of water resources. Since the water value will be dependent on the prospected electricity price and market scenario, it is calculated for medium and long-term scheduling. The water value is then introduced in the short-term hydropower scheduling as a boundary condition, bridging the short and long-term solution strategies [15].

2.2 The Nordic Electricity Market

Since the Nordic countries deregulated their power markets in the 1990s, Nord Pool [21] has served as the main marketplace for wholesale trading of electric power in the region. Since then, the Nordic and Baltic markets have been integrated and now consists of Norway, Sweden, Denmark, Finland, Estonia, Latvia, and Lithuania. Along with this, the market has a strong coupling to the rest of the European electricity market through onshore and sub-sea transmission lines.

The majority of the power trading in the Nordic market is conducted in the Day-ahead market (spot market), where power producers and consumers place bids on their desired volumes of trade for the following day. The *system price*, which is the common Nordic price for each hour in the next 24-hour period, is then determined by *supply and demand*. Since both production and consumption of power can be troublesome to predict a day in advance, there is a need for electricity trading closer to real-time. This need introduces the Intraday market, where power is traded as close as fifteen minutes before delivery. Utilization of this market has proven to be especially beneficial for the trading of power generated by renewable energy sources such as wind and solar, as they suffer from high variability and low predictability [22].

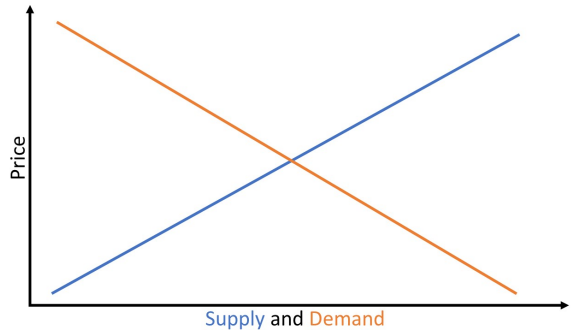

Figure 2.3: *Curve representation of the supply and demand concept.*

As a last measure of balancing the supply and demand of the electricity markets, the Transmission System Operators (TSOs) can up- or down-regulate generating plants participating in the Regulating power market. This market exists to make sure there is balance in the system at all times, and thus ensure frequency stability. Reasons for imbalance can be a wrongful prediction of demand or production, or sudden faults in the system. Depending on the level of regulation, hydropower producers in Norway can get

compensated to participate in this market [23].

The spot market system price is calculated assuming power can flow freely without regard to operational constraints or capacity limitations. However, this is not the case, as the maximum power flow on each line constrains the transmission system. As a result of this, the electricity market is divided into different price zones. The electricity price of each zone can then be calculated by considering the maximum transfer limitations between them. In practice, this means that for two neighboring zones, the zone with a power surplus will have a lower electricity price than the zone with a power deficit [24]. When power has to be transferred between the two zones, the TSO will earn a congestion fee equal to the transferred volume times the difference in electricity price.

2.2.1 The Norwegian Power System

The Norwegian power system is divided into five price areas, as seen in Figure 2.4. The price areas reflect structural bottlenecks and limit the possibility of transferring power from one area to another. Zonal pricing is the main principle of the Norwegian spot market, as an approximation to the nodal pricing scheme. The zonal markets are cleared separately, giving a price for each area [25].

Internal transmission constraints within the price areas are handled through *counter trading*. This implies a common market price, where the TSO buys increments and/or decrements from producers and/or consumers to reduce transmission over the bottlenecks. The TSO must be allowed to pick bids from the regulation list based on the best effect on the relevant bottlenecks. Statnett, the TSO of the Norwegian grid, could compensate for an increase in production/consumption for producers or consumers to relieve the constraint. To minimize the cost of re-dispatching, something to consider in a meshed network is how different agents affect the bottleneck. This may affect the cost for the TSO and the way this cost is charged to the market participants, and the overall efficiency of the market [25].

Figure 2.4: *The five Norwegian price areas [26].*

Roles and responsibilities in the Norwegian power system

The Norwegian energy authorities are responsible for the overall framework for regulating the power grid sector, while the Ministry of Petroleum and Energy has the overall responsibility for the management of energy and water resources in Norway. It is the ministry's task to ensure that the management is carried out according to the guidelines provided by the Norwegian Parliament (Stortinget) and government (Regjeringen). Together with the Norwegian Water Resources and Energy Directorate (NVE), the ministry constitutes the licensing authority for energy facilities in Norway, including the power grid. Within NVE, the Energy Regulatory Authority (RME) is designated to perform the tasks of an independent regulatory authority. Their role is to regulate and follow up on grid companies so that electricity is transferred to the correct delivery quality and price, and that the grid is utilized and developed in a safe and socio-economic manner. Grid companies shall act neutrally towards all grid customers and power suppliers. By imposing an annual revenue limit on the grid companies, the price at which they can sell electricity is restrained. [27]

2.2.2 Price Area NO4

The price area of NO4 covers the area of northern Norway, all the way to the Russian border in the northeast. The current grid is mainly comprised of aging 132 kV transmission lines, along with a continuously expanding 420 kV network. Due to large distances

and old transmission lines, the transfer capacity internally and out of the price zone is relatively low. NO4 borders four other price zones. In the far north, a 220 kV line from Varangerbotn to Ivalo connects the Norwegian and Finish power grid. The 420 kV Ofoten-Ritsem and 132 kV Røssåga-Tornehamn transmission lines connect NO4 to SE1 and SE2, respectively. The connection between NO3 and NO4 consists of both a 300 kV and a 420 kV transmission line, as well as several regional lines operating at lower voltage levels.

Historical data from Nord Pool [21] shows that NO4 has had a net export to other price areas for the last several years. For 2020, the net export was 3.46 TWh to NO3, 1.27 TWh to SE1 and 0.07 TWh to SE2, resulting in an average net export of around 550 MW. Also, the increased exchange capacity to Germany and Great Britain has given new flow patterns and more dominant bottlenecks in the Norwegian power system. While southern Norway (NO1, NO2, NO5) is closely connected to Europe, grid limitations have meant that the northern bidding areas (NO3, NO4) are less influenced by prices in Europe [5]. According to the Norwegian Oil Directorate, implementing new consumption units within the petroleum industry can generate significant socio-economic benefits in the region. However, this, along with the introduction of planned data centers, battery factories, and ammonia factories, intensifies the capacity problem. [26, 28, 29]. In [26, 30], Statnett presents the tentative transmission grid for northern NO4 by 2040, which has been designed to handle an expected consumption increase of 1600-2250 MW in the region. However, it's worth noting that this model is subject to uncertainty.

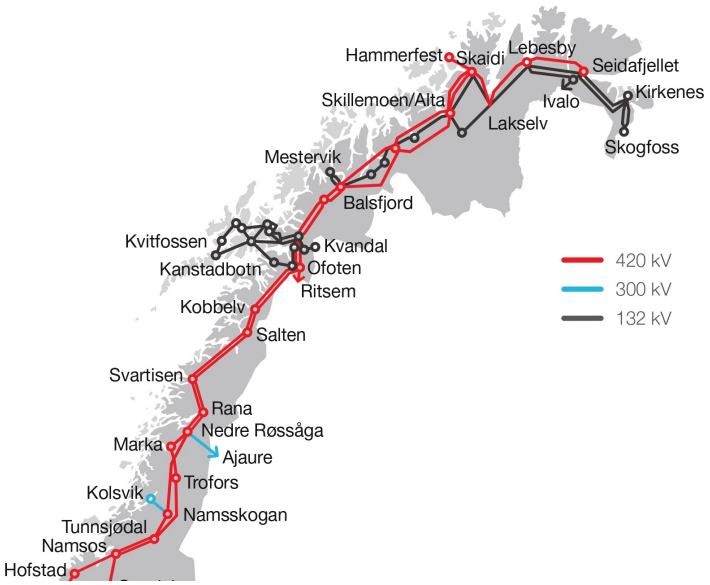

Figure 2.5: *Statnett's prospect for the northern NO4 transmission grid in 2040 [26].*

2.3 Power Transfer Distribution Factors

Power Transfer Distribution Factors (PTDF) can be used to quickly calculate the change in flow on a line due to power injection on a bus. This tool can be helpful for both congestion and contingency analysis in a system. The DC power flow assumptions made when calculating PTDF enable these factors to be used to express transmission line capacity constraints in *Short-Term Hydro Scheduling*, which is further covered in section 2.3.1. This chapter will begin by introducing an efficient method for calculating PTDF, and then delve into the various practical applications they have.

The use of *Power Transfer Distribution Factors* assumes a change in power injection from one bus to another. The PTDF gives the fraction of that transferred power injection that ends up flowing on line l_{ij}. To define the distribution factors, let's first look at the DCPF equations in (2.6) and (2.7), where $\Delta\theta$ is the voltage angles and $\boldsymbol{B'}$ is the $Ybus$ with line resistances neglected. X_{ij} is the line reactance and F_{ij} is the power flow between i and j.

$$\Delta\theta = \boldsymbol{B'}^{-1}\boldsymbol{P} = \boldsymbol{X}\boldsymbol{P} \tag{2.6}$$

$$F_{ij} = \frac{\theta_i - \theta_j}{X_{ij}} \tag{2.7}$$

Equation (2.6) can then be partitioned to get θ_i and θ_j:

$$\theta_i = x_{i1}P_1 + x_{i2}P_2 + x_{i3}P_3 + \ldots + x_{in}P_n \tag{2.8}$$

$$\theta_j = x_{j1}P_1 + x_{j2}P_2 + x_{j3}P_3 + \ldots + x_{jn}P_n \tag{2.9}$$

Inserting (2.8) and (2.9) into (2.7):

$$F_{ij} = \frac{(x_{i1} - x_{j1})}{X_{ij}}P_1 + \frac{(x_{i2} - x_{j2})}{X_{ij}}P_2 + \frac{(x_{i3} - x_{j3})}{X_{ij}}P_3 + \ldots + \frac{(x_{in} - x_{jn})}{X_{ij}}P_n \tag{2.10}$$

$$F_{ij} = a_{ij,1}P_1 + a_{ij,2}P_2 + a_{ij,3}P_3 + \ldots + a_{ij,n}P_n \tag{2.11}$$

By definition [31, 32], the distribution factor $a_{ij,b}$ for line l_{ij} with change in power at bus b is then given in Equation (2.12):

$$a_{ij,b} = \frac{(x_{ib} - x_{jb})}{X_{ij}} \tag{2.12}$$

The PTDF factors are linear estimates of the change in flow on a line with a shift in power from one bus to another. These factors depend on the choice of the balancing nodes, topology, and network parameters, but are independent of the injection and power flow through the system [32, 33]. Equation (2.11) demonstrates the relationship between the summation of $a_{ij,b} \cdot P_b$ across all buses and the power flow on line l_{ij}. This implies that by employing a complete set of PTDF factors and power balances, the entire power flow in a system can be quickly calculated. Equation (2.13) shows a full PTDF matrix, where rows correspond to lines and columns correspond to buses.

$$PTDF = \begin{bmatrix} a_{bus1}^{line1} & a_{bus2}^{line1} & \cdots & a_{busM}^{line1} \\ a_{bus1}^{line2} & a_{bus2}^{line2} & & \\ \vdots & & \ddots & \\ a_{bus1}^{lineN} & & & a_{busM}^{lineN} \end{bmatrix} \tag{2.13}$$

It is important to note that in Equation (2.13), the column corresponding to the reference bus will only consist of zeros. The reason for this is that a change in power at the reference bus will be balanced by the bus itself, and thus not induce a change in flow in the system.

2.3.1 PTDF with fast calculation of inverse elements

Calculation of the PTDFs can be done in numerous ways. As several of these methods require computationally heavy matrix inversions, a method revolving around the fast calculation of inverse matrix elements can be utilized. This method introduces a way to find specific elements of an inverse matrix, allowing for the calculation of individual PTDF factors without inverting the full network impedance matrix. This method is especially

useful in contingency analysis, where the calculation of PTDF factors for all lines may be excessive [34]. It must be noted that this method is neither new nor specific to the field of electrical engineering. It is simply a mathematical method used to efficiently calculate specific elements of an inverse matrix. As contemporary research on power flow analysis is often more focused on the overall efficiency of comprehensive, full-package power system simulation tools, the mathematical method is not commonly mentioned. However, this method has been utilized in power system analysis, particularly for contingency analysis, as far back as 1974 [35].

$$\boldsymbol{B'}a = b \tag{2.14}$$

In Equation (2.14), $\boldsymbol{B'}$ is the same $Ybus$ as in (2.6), with rows and columns correlating to the reference bus removed. By manipulating the b-vector and solving for a, the PTDF factors for the line in question can be found.

The first step in this alternative approach is to determine for which line the PTDF is to be calculated, and whether this line is connected to the reference bus or not. This distinction is important for establishing the matrix equations to be used in the fast calculation of inverse elements. Based on this, two different possibilities with respective matrices of linear equations can occur;

1. The line is connected from bus i to the reference bus j:

$$\begin{bmatrix} B_{11} & B_{12} & \cdots & B_{1n} \\ B_{21} & B_{22} & & \\ \vdots & & \ddots & \\ B_{n1} & & & B_{nn} \end{bmatrix} \begin{bmatrix} a_1 \\ a_i \\ \vdots \\ a_n \end{bmatrix} = \begin{bmatrix} 0 \\ \frac{1}{X_{ij}} \\ \vdots \\ 0 \end{bmatrix} \tag{2.15}$$

   Note: If the line is defined from *reference bus j* to *bus i, the b-vector is multiplied with -1.*

2. The line is connected from bus i to bus j, non of which are the reference bus.

$$\begin{bmatrix} B_{11} & B_{12} & \cdots & B_{1n} \\ B_{21} & B_{22} & & \\ \vdots & & \ddots & \\ B_{n1} & & & B_{nn} \end{bmatrix} \begin{bmatrix} a_i \\ a_j \\ \vdots \\ a_n \end{bmatrix} = \begin{bmatrix} \frac{1}{X_{ij}} \\ -\frac{1}{X_{ij}} \\ \vdots \\ 0 \end{bmatrix} \tag{2.16}$$

Note: If the line is defined from *bus j* to *bus i, the b-vector is multiplied with -1.*

After establishing the b-vector, the equation system is solved by using forward and backward substitution [36]. By doing this, the computational-heavy full matrix inversion is circumvented. A practical implementation of this solution strategy is presented in Section 3.4

PTDF in STHS

As mentioned before, the STHS optimization problem consists of an objective function, decision variables, and operational constraints. In addition to quickly calculating the change in power flows due to a shift in power distribution, *Power Transfer Distribution Factors* can be used to express constraints for the maximum transfer capacities of the individual transmission lines. This is shown in Equation (2.17). Incorporating this constraint into the optimization process of STHS ensures that the power distribution generates power flows within the maximum transfer capacities.

$$-F_{ij}^{MAX} \leq \sum_{bus=1}^{n} a_{ij,bus} P_{bus} \leq F_{ij}^{MAX} \tag{2.17}$$

Power losses on lines can also be taken into account when solving a linear optimization problem with PTDF. The DC power flow is by definition lossless, but the loss can be modeled and included in the PTDF line flow constraints in (2.17). In [37], the DCOPF problem is modeled with and without losses. If line losses are to be considered, P_{ij}^{loss} will be split equally to the sending bus i and receiving bus j. This allocation logic is derived from the principles of DC power flow, where the voltage V is assumed to be 1 per unit (p.u.). In this simplified model, the power loss P_{ij} is equal to the magnitude of the current I_{ij} flowing through the transmission line. As a result, the loss P_{ij}^{loss} is evenly divided between the two ends of the line, i.e., the sending bus i and the receiving bus j. Line losses can be added to Equation (2.17) by considering Equation (2.18).

$$a_{ij,bus} P_{bus} = a_{ij,bus} (P_{bus}^{lossless} - \frac{1}{2} P_{ij}^{loss}) \qquad \text{for } bus = i, j \tag{2.18}$$

PTDF in contingency analysis

Line outages in an electric grid frequently lead to unfavorable operating conditions. When a line experiences a fault, the power flow must be redistributed among other lines,

potentially resulting in overload of transfer capacities. In order to either prevent these conditions or rectify them once they occur, contingency analysis plays a crucial role. The DC approximation and its associated *Power Transfer Distribution Factors* are valuable tools in contingency analysis, as they provide useful insights without requiring precise calculation of complete AC power flow.

Line Outage Distribution Factors (LODF) serve as an adapted version of PTDF, primarily employed as a preemptive measure before encountering contingencies. The LODF factors are utilized to see how the power flow would be distributed in the system if one or more transmission lines were experiencing outages. The LODF calculation process closely resembles that of PTDF. Figure 2.6 shows the implementation of this technique. The procedure starts with an initial line flow in the system, caused by the initial generation schedule and load. To prevent transmission line overloads resulting from an outage on line ij, the corresponding row and column pertaining to line ij are eliminated from the $\boldsymbol{B'}$-matrix in Equation (2.14). Calculating new line flows according to Equation (2.17) will reveal any potential capacity overload. If this is the case, the initial flows must be adjusted accordingly. [38]

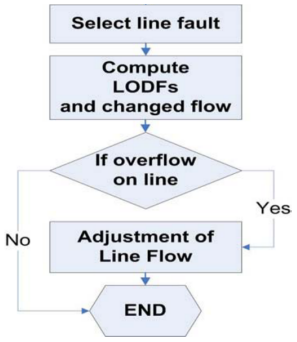

Figure 2.6: *LODF contingency prevention. Figure adapted from [38]*

By employing the LODF technique for contingency analysis, a new set of PTDF and optimization constraints are generated for each case of line outage, which can drastically increase the computational time of the optimization problem. A solution is to utilize Benders Decomposition — a powerful decomposition method that enables the division of the optimization problem into smaller, more manageable components. Benders Decomposition consists of a master problem that handles the primary optimization task, while sub-problem optimizations address each line outage scenario. The results from solving

each sub-problem are subsequently analyzed and incorporated iteratively as constraints into the master problem. This iterative process ensures consideration of all line outage scenarios while maintaining computational efficiency. The following procedure, along with the simplified flowchart in Figure 2.7 explains how Benders Decomposition can be utilized in contingency analysis. [39]

1. Formulate and solve the master problem to obtain an initial solution.
2. Formulate and solve the first sub-problem while using fixed variables from the initial solution.
3. Analyse the solution of the sub-problem and update the master problem by incorporating new constraints based on the sub-problem solution.
4. Interchanging between solving the updated master problem an sub-problems, iterate through each contingency scenario. Each iteration refines the solution and adds security constrains for the given contingency scenarios.

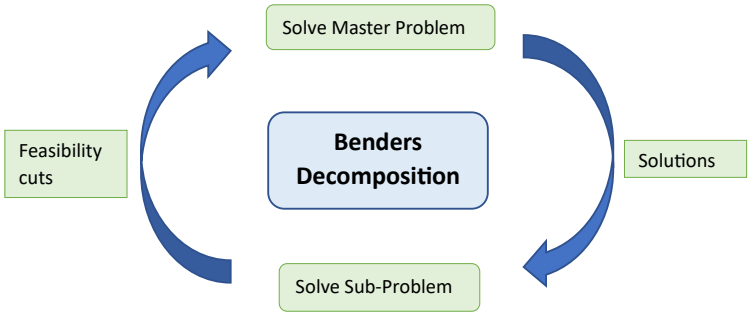

Figure 2.7: *Simplified flowchart for Benders Decomposition.*

PTDF attributes

One notable advantage of PTDF is its ability to streamline calculations by focusing on smaller areas within a network. By leveraging the knowledge of export/import patterns for a specific region, it becomes unnecessary to calculate distribution factors for the entire network. This approach allows for a more targeted analysis, as the attention can be solely directed towards the smaller area, resulting in efficient calculations. The methodology described has a notable limitation: its applicability is restricted to a specific export/import scenario. This constraint arises from the fact that even minor fluctuations

in power within the broader network can impact numerous buses within the smaller region. However, techniques are available to mitigate this issue, such as employing PTDF equivalents. The PTDF equivalent method allows the nodes within an area to be represented by a single node, by calculating an equivalent set of distribution factors according to Equation (2.19). Here, P_0 is the initial power balance distribution in the system.

$$a_A^{ij} = \frac{\sum_b (a_b^{ij} \cdot P_{0,b})}{\sum_b P_{0,b}} \qquad \text{for all buses } b \text{ in area } A \tag{2.19}$$

This equation gives the PTDF factor a^{ij} for line l_{ij} with regard to total change in power within area A. It is important to note that the PTDF equivalents only hold validity under the assumption that all units are regulated according to the initial distribution. To obtain a reduced PTDF matrix, a specific procedure can be followed. First, the rows corresponding to lines within area A are eliminated from the original PTDF matrix. Then, the columns corresponding to buses in area A are replaced with a new column computed using Equation (2.19). [40]

2.3.2 Day-ahead network modeling

Various methods for day-ahead market clearing are utilized around the world. The Nordic electricity market, along with most of Europe, adopts the zonal pricing model. The nodal pricing approach is favored by countries such as the US and New Zealand [41]. The different market clearing methodologies are an interesting topic for discussion, particularly about PTDFs and their impact on the clearing process. The following paragraphs provide insights into different market clearing methodologies, namely *Flow-Based Market Coupling* (FBMC) and *Available Transmission Capacity* (ATC), their impact on social welfare and grid optimization, and how they compare to the nodal approach.

Flow-Based Market Coupling uses the physical transmission constraints of the electrical network, considering PTDFs. The PTDF matrix and *remaining available margin* (RAM) determine the feasibility region at any given time. With FBMC it is theoretically possible that power flows from a high-price area to a low-price area if it increases social welfare. FBMC models the electrical network, considering cross-border exchanges including

security constraints. The main objective for FBMC is then to optimize market flows and social welfare [42].

The Nordic countries have utilized *Available Transmission Capacity* as their capacity methodology up until now. It measures the maximum capacity for commercial exchange across a given border in one direction. However, this approach is typically more limiting than FBMC due to its simplified modeling that neglects electrical characteristics. Additionally, PTDFs are not included in the market algorithm when using ATC. The algorithm focuses on the total capacity available at each border. As a result, using ATC typically gives lower social welfare due to the limited transmission capacity available [42, 43]. Similar to FBMC, ATC aims to maximize social welfare. The possible solution domain for the two methodologies can be seen in Figure 2.8a for the simple three-node system in Figure 2.8b, with equal line impedance and capacity.

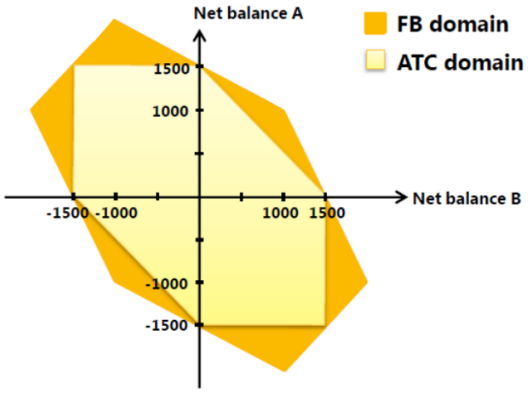

(a) *ATC and FBMC domains in a simple three-node system. Adapted from [43]*

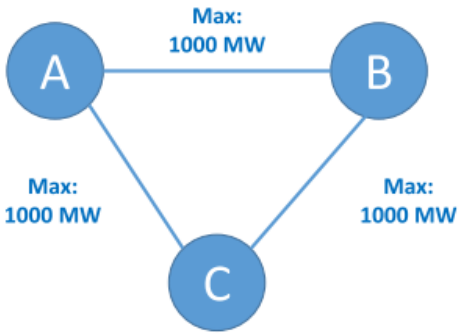

(b) *Three-node system.*

Figure 2.8: *FBMC and ATC approach.*

Among the three models illustrated in Figure 2.9, the nodal pricing model needs the most detailed information regarding the grid topology. All elements are taken into account in the model. The laws of physics are applied to the whole network, and line flows are restricted by thermal capacities. In FBMC, the laws of physics are only applied to the Critical Branches (CBs), while the other lines have no physical restrictions. The CBs could be lines connecting two price areas or lines within a price area. The ATC model is illustrated furthest right in Figure 2.9. In the ATC model, only the power transfer

between the price areas is limited. No physical restrictions are applied to lines within a price area. Solutions given by the ATC model do not guarantee a congestion-free network. Hence, re-dispatching may be needed, which incurs extra costs [44].

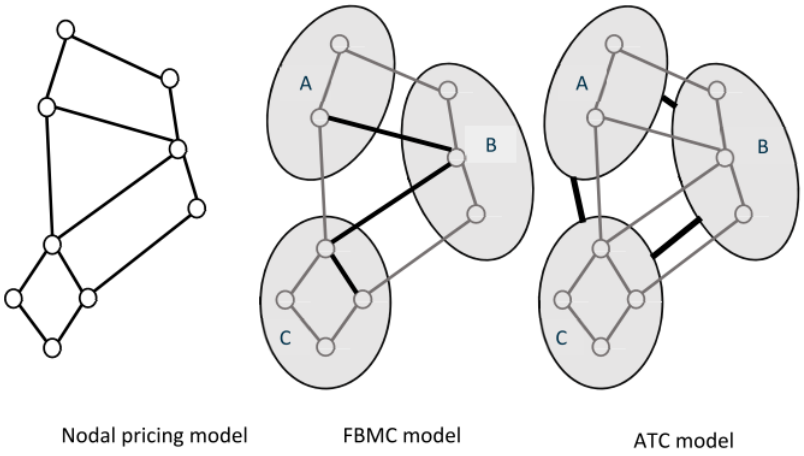

Figure 2.9: *Day-ahead market models [44].*

2.4 SHOP

Short-term Hydro Optimization Program (SHOP) is an STHS tool developed by SINTEF ER, and is used by most large hydropower producers in the Nordic countries for daily operations. The conventional use of SHOP is for a customer to optimize one or several hydro systems within the same price zone. The optimization is often with regards to expected market price, and grid limitations are typically not considered. After the market has been cleared and the producer knows how much to produce, optimization can be done with regard to load obligations. The key objective of SHOP is to maximize profit, assuming market prices and inflows are known during the planning horizon. SHOP uses mixed-integer linear programming (MILP) and linear programming (LP) to solve the optimization problem. The problem is decomposed into two modes: *unit commitment mode* (UC) and *unit load dispatch mode* (ULD) [12, 17].

The first stage of the solution strategy in SHOP is the UC mode, as seen in Figure 2.10. Here, the iterations are performed to stabilize head variation in the reservoirs. The volume and water level of the reservoirs are updated after each iteration. Then the convergence criterion is checked. If the value is smaller than a given tolerance, the

iterative process finishes. In the UC mode, a MILP model is solved to specify the on/off decision for each unit per period. The convergence criterion is typically met after three to five iterations. After this, the ULD mode is activated. The model transitions into pure LP and determines a dispatch schedule regarding the generation level for each committed unit after two or three iterations [13, 17].

SHOP utilizes detailed descriptions of reservoirs, gates, junctions, plants, and generating units as its primary inputs. Examples of SHOP inputs can be found in Appendix A. The optimization problem in SHOP is given a set of constraints. These constraints encompass a range of considerations, including limitations on the maximum rate of change for different production units, constraints on reservoir levels (both minimum and maximum), and coupling with medium-term scheduling, including water values. The outcome of the optimization process is the determination of the optimal dispatch for each generator within the system. In addition to the dispatch, a range of calculated data is generated during the optimization process. The main outputs include reservoir trajectories, water flow, plant and unit dispatch schedules, and optimal distribution of reserves among units [45]. These outputs can be extracted and utilized for further analysis and decision-making.

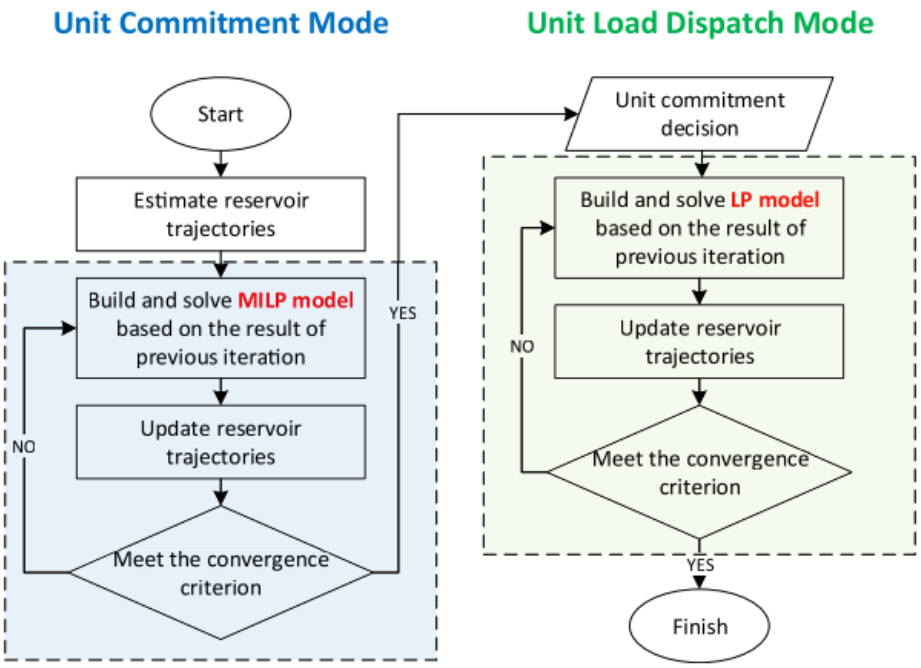

Figure 2.10: *Solution strategy in SHOP [17].*

3 Methodology & Materials

The SHOP system model utilized in this thesis is developed based on both classified and openly available data. In this chapter, the system model, topology, and optimization problem is introduced. For further details, please refer to Appendix A - F.

3.1 System model

To demonstrate the applications of *Power Transfer Dirstribution Factors* (PTDF) in *Short-Term Hydro Scheduling* (STHS), simulations were conducted using the SHOP platform. These simulations were based on a consistent foundation and set of parameters. The optimization period selected for analysis was the first week of 2022, spanning from January 1st at 00:00 to January 8th at 00:00. The choice of the first week of January is particularly compelling for *Short-Term Hydro Scheduling* due to several factors. As this period coincides with the winter season, there is typically a higher electricity demand, driven by the need for heating. Consequently, the water levels in hydropower reservoirs tend to be high during this time, offering ample resources to meet the heightened demand. [5]

The specific area of interest for this study is NO4, the northernmost price zone in Norway. This choice was based on the radial configuration of the transmission grid in this region, which offers distinct advantages for the simulation. The radial nature of the grid simplifies the analysis of line flows, making it easier to comprehend and interpret the results. A radial structure also makes the transmission grid vulnerable to line outages, which makes NO4 an ideal area for conducting contingency analysis.

A dataset produced by Statkraft, containing 16 hydropower plant SHOP models, laid the foundation for deciding which NO4 power plants to include in the simulation. The models contain all of the static data associated with hydropower stations. To accurately represent the hydropower plants in the SHOP simulation, additional information such as reservoir inflow, reservoir start head, and water value was required. Moreover, to conduct the power flow analysis aspect of the simulation, data on the transmission grid topology, characteristics, and electricity demand curves for the specified period were also essential inputs. Since not all NO4 power production facilities are represented in the

dataset, excluded plants were emulated in a specific way. How this was accomplished is explained in Section 3.3.

Transmission grid data was provided in a dataset from NVE. Each hydropower plant was connected directly to the nearest accessible transmission line in the data set. These connection points formed the distribution of nodes to be used in the simulation. It was assumed that the power flow capacities of the lines connecting the power stations to the transmission grid were already sufficient. Consequently, excluding this specific aspect from the simulation, focusing instead on the scheduling of the hydropower plants within the context of the transmission grid. This assumption was grounded in an assessment conducted by Statnett, which determined that the regional grid of NO4 can accommodate a moderate increase in power demand. [28]

3.1.1 Case 1 - Base case

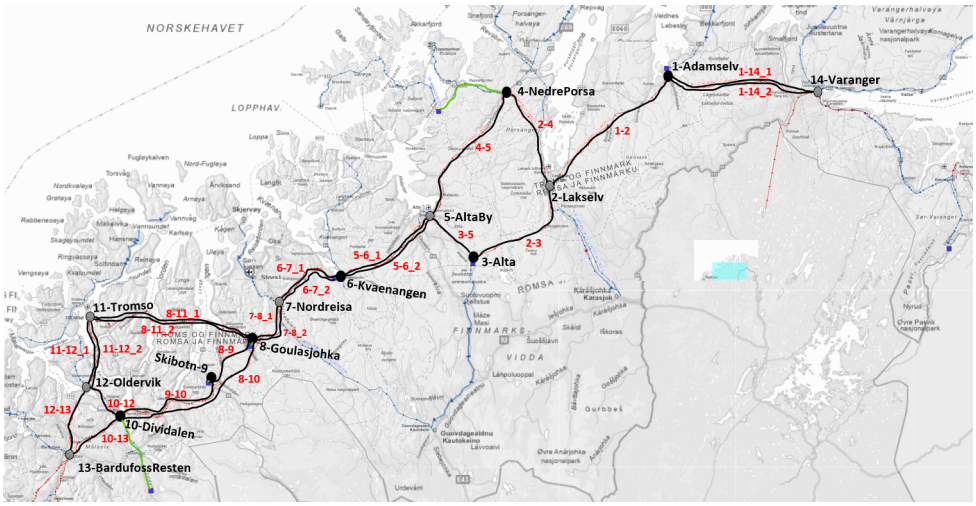

Figure 3.1: *Simplified topology for Case 1*

Based on the data provided, a topology with 14 buses and 23 transmission lines was selected for the base case scenario (Figure 3.1). In the northern region, the system extends to the Russian border through Bus 14, called *Varanger*. This bus facilitates power exchange with the Finnish grid. In the south, Bus 13, referred to as *BardufossResten*, serves as an aggregated bus for the remaining portion of the NO4 price zone. The need for an aggregated bus like Bus 13 arises due to the background data, which often covers the entire NO4 region. A notable example is the load demand data, which is available in

its entirety on Nordpool [21]. The aggregated bus serves as a central point to incorporate the complete load demand for southern NO4 and facilitate exchange with connected price zones effectively.

The network consists of four loops, with an otherwise radial structure. There are several parallel lines within the network, respectively between *Adamselv* and *Varanger*, *AltaBy* and *Kvaenangen*, *Kvaenangen* and *Nordreisa*, *Nordreisa* and Goulasjohka, Goulasjohka and Tromso, and finally between Tromso and *Oldervik*. Out of the 14 buses, 7 buses contain hydropower SHOP models used in the simulation. These are marked with black dots in Figure 3.1 and displayed in Table 3.1. Bus 1, *Adamselv*, is designated as the balancing bus within the system. Although the choice of *Adamselv* as the balancing bus influences the PTDF calculations, it does not introduce any changes to the overall outcomes of the simulation.

Table 3.1: *Case 1 system data.*

Bus	Hydropower SHOP model	Other available power, max [46, 47]	Load demand + export, mean
1 - Adamselv	Adamselv - 52.8 MW	Wind: 39 MW, Hydro: 4.4 MW	1.0 MW
2 - Lakselv			36.9 MW
3 - Alta	Alta - 166 MW		15.3 MW
4 - NedrePorsa	Nedre Porsa - 12.4 MW	Wind: 41 MW, Hydro: 4.4 MW	96.6 MW
5 - AltaBy		Hydro: 9.0 MW	101.1 MW
6 - Kvaenangen	Kvænangsbotn - 81 MW	Hydro: 30.3 MW	66.8 MW
7 - Nordreisa		Hydro: 8.2 MW	0.0 MW
8 - Goulasjohka	Goulasjohka - 80 MW	Hydro: 7.7 MW	9.4 MW
9 - Skibotn	Skibotn - 72 MW	Hydro: 19.1 MW	3.3 MW
10 - Dividalen	Dividalen - 26 MW		45.5 MW
11 - Tromso		Wind: 335 MW, Hydro: 38.0 MW	179.1 MW
12 - Oldervik			4.0 MW
13 - BardufossResten		Wind: 582 MW, Hydro: 4720 MW	3383.1 MW
14 - Varanger		Wind: 148 MW, Hydro: 74.4 MW	231.6 MW

3.1.2 Case 2 - Line outage

The objective of Case 2 is to illustrate the practical application of PTDFs in calculating line flows, either during or before a line outage. Line 3-5 between *Alta* and *AltaBy* was chosen for the outage, due to it being part of one of the loops in the system. Simulating

the outage can be effectively accomplished by manipulating the PTDF calculation. This involves the straightforward process of removing the row in the input data that corresponds to line 3-5 in the PTDF module, as detailed in Section 3.4. Given the pivotal role of PTDF in the optimization problem, the resultant effect will be the elimination of any flow on line 3-5. This strategic manipulation of PTDF data allows for a simulated representation of the outage scenario and facilitates the analysis of system behaviour and flow distribution under such conditions. Except for this specific modification, all other parameters remained unchanged from Case 1.

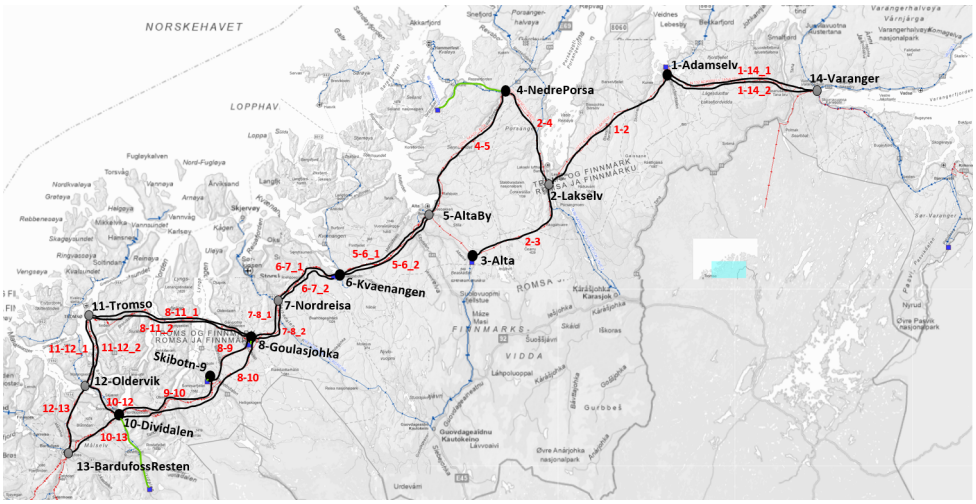

Figure 3.2: *Simplified topology for Case 2 with outage between Bus 3 and 5.*

3.1.3 Case 3 - Reduced model

Case 3 exemplifies a key attribute of PTDF, which allows for streamlined calculations by directing attention to smaller areas within a larger network. For this case, a reduced model was utilized, specifically targeting the region spanning from Bus 6 (*Kvaenangen*) to Bus 14 (*Varanger*). To emulate the export and inflow patterns of this particular area, the line flows between Bus 6 and Bus 7 from Case 1 were integrated into Bus 6 as an additional load. Subsequently, the PTDF calculations were updated by excluding the unnecessary buses and lines from the input file of the PTDF module, much like what was done in Case 2. Apart from these changes, all other parameters remained unchanged from Case 1. The reduced model is shown in Figure 3.3.

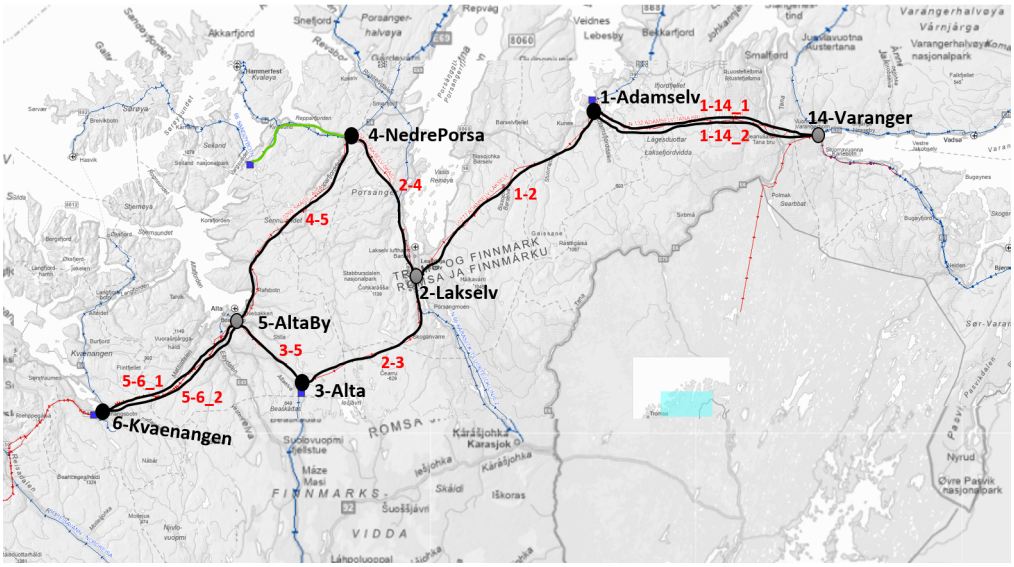

Figure 3.3: *Simplified topology for Case 3 - reduced model.*

3.2 SHOP Optimization Problem

As described in Section 2.1.2, the STHS optimization problem comprises an objective function and a set of constraints. This section provides a detailed explanation of the objective function in SHOP and highlights some constraints that are essential to the STHS problem. The same constraints and notations can be found in Ref. [1]. While not all constraints used in the SHOP optimization are listed below, the most significant ones are included. A more comprehensive analysis of the constraints was done in the specialization project [13].

The optimization problem in SHOP can be formulated as:

$$\text{Min} \sum_{t\in T}\sum_{s\in S}\sum_{i\in I_S} q_{i,s,t} - \sum_{k\in K} W_{k,t}^{END}\cdot E_S \cdot v_{k,t} + \sum_{s\in S}\sum_{i\in I_S} C_{i,s}\cdot \mu_{i,s,t} + C_{i,s}^{PEN}\cdot \beta \qquad (3.1)$$

Subject to:

$$p^G_{i,s,t} = G \cdot \eta^{GEN}_{i,s}(p_{i,s,t}) \cdot \eta^{TURB}_{i,s}(h^{NET}_{i,s,t}, q_{i,s,t}) \cdot h^{NET}_{i,s,t} \cdot q_{i,s,t} \tag{3.2}$$

$$P^{MIN}_{i,s} \cdot \omega_{i,s,t} \leq p^G_{i,s,t} \leq P^{MAX}_{i,s,t} \cdot \omega_{i,s,t} \tag{3.3}$$

$$Q^{MIN}_{i,s,t}(h^{NET}_{i,s,t}) \cdot \omega_{i,s,t} \leq q_{i,s,t} \leq Q^{MAX}_{i,s,t}(h^{NET}_{i,s,t}) \cdot \omega_{i,s,t} \tag{3.4}$$

$$V^{MIN}_k \leq v_{k,t} \leq V^{MAX}_k \tag{3.5}$$

$$q^{TOTAL}_{k,t} = \sum_{i \in I_S} q_{i,s,t} + q^{BYPASS}_{k,t} \tag{3.6}$$

$$0 \leq q^{BYPASS}_{k,t} \leq Q^{BYPASS\_MAX}_k \tag{3.7}$$

$$p^G_{n,t} - p^D_{n,t} = \sum_{j \neq i} p_{t,ij} \tag{3.8}$$

$$-F^{MAX}_{ij} \leq \sum_{bus=1}^{n} a_{ij,bus} \cdot P_{bus} \leq F^{MAX}_{ij} \tag{3.9}$$

Objective function

The objective function in SHOP will depend on the system model and is therefore unique for each problem. The optimization problem searches for the most economical schedules among the generating units while accounting for constraints and penalty variables [13]. The first term in Equation (3.1) minimizes the water discharge of unit i in plant s in period t ($q_{i,s,t}$). The second objective is to minimize water utilized by turbines or spilt. Water value $W^{END}_{k,t}$ refers to the opportunity cost of storing water for later production versus using it now. $W^{END}_{k,t}$ is given in $[\frac{€}{MWh}]$, and an energy conversion factor E_S is needed to build an energy conversion [1]. $W^{END}_{k,t}$ are also one of the main coupling signals used in STHS for coupling to long-term/mid-term scheduling. This has not been investigated, as it is not part of the scope of the thesis. The third term minimizes the start-up and shut-down costs of units ($C_{i,s}$) based on the start-up decision of unit i in plant s during period t. Additionally, penalty variables ($C^{PEN}_{i,s}$) are included, multiplied by a general penalty variable, β.

Power production and water discharge

Equation (3.2) defines the relationship between water discharge (input) and electrical energy (output). The power output is dependent on the generator and turbine efficiency ($\eta_{i,s}^{GEN}$ and $\eta_{i,s}^{TURB}$), net head ($h_{i,s,t}^{NET}$), water discharge ($q_{i,s,t}$) and conversion constant of gravity acceleration and water density (G). Equation (3.3) determines the lower and upper output power limits of the generator ($P_{i,s}^{MIN}, P_{i,s}^{MAX}$), while Equation (3.4) corresponds to the permissible discharge range of the turbine ($Q_{i,s,t}^{MIN}(h_{i,s,t}^{NET}), Q_{i,s,t}^{MAX}(h_{i,s,t}^{NET})$).

Water balance and storage limits of reservoirs

Equation (3.5) restricts the allowable water volume of the reservoir within minimum and maximum water limits. Equation (3.6) is the total regulated water release of reservoir k in period t ($q_{k,t}^{TOTAL}$) equal to the sum of water discharge of unit i and water release via the bypass gate of reservoir k. The maximum controllable spillage of reservoir k is restricted in Equation (3.7).

Power flow constraints

Equation (3.8) balance the production and consumption in node n with the sum of power flow on the connected transmission lines. Equation (3.9) restricts the allowed power flow on each branch (F_{ij}^{MAX}) given by the PTDFs ($a_{ij,bus}$). Details regarding power flow constraints are further explained in Section 3.4.

3.3 Data construction

This section presents important input values needed for the optimization of the STHS problem.

3.3.1 Line data

A set of data was provided by NVE containing information about line reactance and capacity. A number of lines, including 420 kV transmission lines constructed after 2020, are not given in the dataset. When line data was not available, simplifications were made. Information about the different transmission lines and assumptions utilized for the SHOP simulations can be found in Appendix D.

3.3.2 Inflow

Information regarding inflow was gathered from the website NVE Atlas [48]. Water inflow uncertainty is neglected in this deterministic STHS model. The natural inflow into reservoir k in period t is given as $Q_{k,t}^{NI}$ and converted from $[\frac{Mm^3}{year}] \rightarrow [\frac{m^3}{s}]$. This is found by selecting the precipitation field for each of the reservoirs using the map function in NVE Atlas. For each field, Q_{NORMAL} is given in $[\frac{Mm^3}{year}]$ based on the median total inflow from 1961 until 1990. Some unregulated rivers do not contain annual inflow data for recent years, like Trollvikelva, close to Goulasjavri. In these cases, the most recent annual inflow data was used. The data was constructed in the following way:

1. Annual median inflow based on Q_{normal} was found at NVE Atlas for each reservoir closest to the precipitation field.
2. The nearest unregulated watercourse containing inflow data at NVE Sildre was used for the calendar year 2022 or the latest published data. The median annual inflow was then used for $Q_{unregulated}$ given in $[\frac{m^3}{s}]$, before converting it to $[\frac{Mm^3}{year}]$.
3. The scaling factor is calculated as follows: $K = \frac{Q_{normal}}{Q_{unregulated}}$. This factor is then multiplied with inflow data from the 1st of January to the 8th of January 2022, before implementing it into the yaml-file for SHOP for $Q_{k,t}^{NI}$ given in $[\frac{m^3}{s}]$.

3.3.3 Power station data

The SHOP models for the power stations utilized in the simulations were created by Statkraft and primarily rely on publicly accessible information. They incorporate all the static data associated with hydropower stations, such as topology, PQ curves, reservoir data, loss data, and generator data. Although the models contain most of the essential information about the power stations, the data set is incomplete and only contains a subset of NO4 power stations. Since there is no available complete power station data for the entirety of NO4, several aspects regarding load and production must be considered, further explained in Section 3.3.5.

The SHOP models capture vital information about the topology of the hydropower plants, emphasizing the interconnections between its various objects. An example of such a topology can be observed in Figure 3.4, showcasing the layout of one of the plants from

the dataset, specifically Adamselv. When combined with data for the individual objects in the model, this information enables the construction of the complete hydropower models. Some of the different object types within the models are reservoirs, generators, turbines, penstocks, gates, and more. Below is a more comprehensive explanation of some of the crucial information that is included in the models.

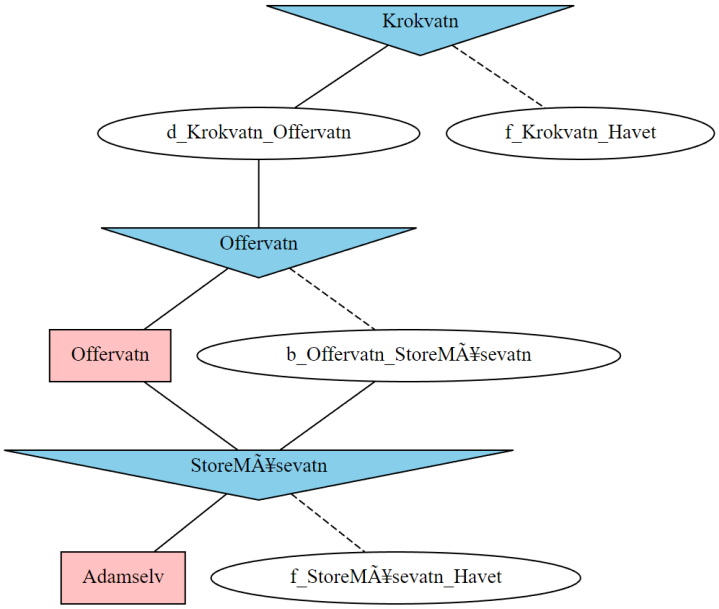

Figure 3.4: *Example of power plant topology.*

Two important variables impacting hydropower production are the generator and turbine efficiency. In SHOP, the turbine efficiency curves provided by Statkraft are described by Hill curves, composed of a set of triples relating to the turbine's net head and discharge rate. Figure 3.5 illustrates the head-dependent turbine and generator efficiency used in the optimization. Although the data points in SHOP may vary between generators and turbines, they typically resemble those depicted in Figure 3.5.

Three main types of flow-related head losses are included in the data set. This is the main loss, penstock loss and tailrace head loss. The main loss and penstock losses are modelled as constant factors, and is related to the friction of water. The tailrace is modelled as an additional head loss curve related to the discharge of the plant. If power loss would have been the main focus of this thesis, the objective would have been to minimize losses in the hydro generation process. More specifically, this would be from tailrace elevation, main

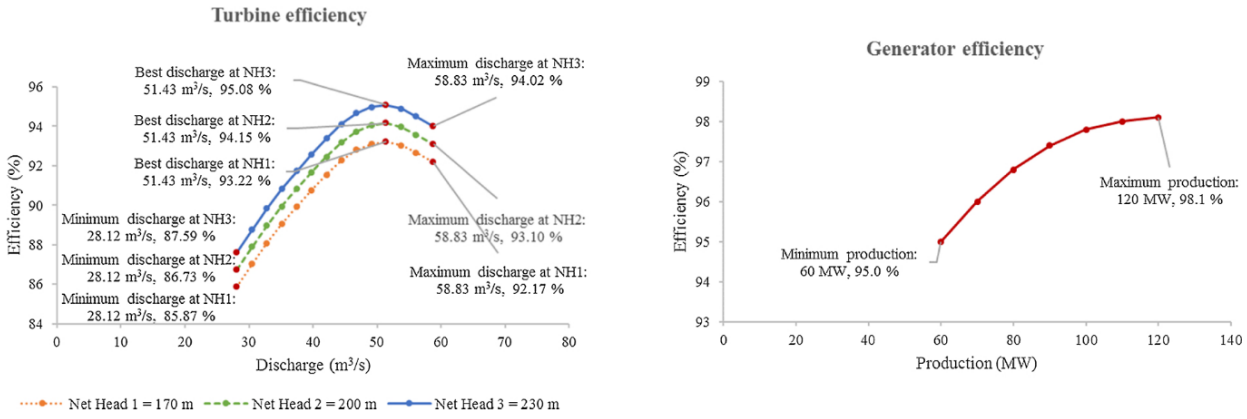

Figure 3.5: *Turbine and generator efficiency curves used in SHOP. Figure adapted from [1]*

head loss, penstock loss and efficiencies in generators and turbines. Even though the objective is to minimize the value of water utilized by turbines or spilt, the parameters are still affecting the SHOP optimization. From [17], it is clear that the penstock losses cannot be ignored. It corresponds to the largest share of the total losses, and will influence the dispatch scheduling even if it accounts for a small percentage of the gross head.

3.3.4 Water value

As mentioned in Section 2.1.5, there are several methods for calculating water values, and as stated, having dependent water values is the theoretically preferred solution. The term "dependent water values" refers to the idea that the value of water in hydropower production is not solely determined by the anticipated water usage from a single reservoir, but rather is influenced by the combined effects of all the reservoirs and hydropower production in the system. Unfortunately, calculating dependent water values is complex and requires sensitive data that hydropower producers keep confidential. As a result, and because the focus on this thesis is not on water value calculation, a simpler method is utilized, namely the Capacity Factor Method [49].

Capacity factor is a term used for several energy production technologies. For a given period, it describes the ratio between the actual produced energy and the amount of energy that would have been produced if the plant was operating at maximum capacity for the entire period. For hydropower plants, this ratio is normally around 30-60%, with

a worldwide average of 44% [50]. The idea behind the Capacity Factor Method is that plants with a high operating time will have a lower water value, as they utilize larger quantities of water, relative to the reservoir size. Plants with lower operating times will have a higher water value, as they use less water and thus have to value it higher. The water values were calculated according to the list below.

$$h_{max} = 8760 \cdot C_f = 8760 \cdot \frac{E_{annual}}{8760 \cdot P_{rated}} = \frac{E_{annual}}{P_{rated}} \tag{3.10}$$

Execution:

1. Production data for Norwegian hydropower plants can be found in NVE's hydropower database [46]. Maximum capacity operating hours h_{max} was calculated according to Equation (3.10), using the average annual energy production and rated power of the plant. It is assumed that the whole-year Capacity Factor C_f also is eligible for the first week of January.
2. Electricity price data for NO4 was downloaded from NordPool [21] with time steps of one hour. The Capacity Factor Method typically uses historical data for the period in question, but to avoid decisive anomalies and allow for smoother regression, a longer time period (January 2022 to June 2022) was used. Another option would be to use historical data and calculate the average price curve for the first week of January, however this could also prove to be deceiving, as electricity prices exhibit a significant degree of variability from one year to the next.
3. The price curve was sorted from high to low and placed along an x-axis ranging from 0 to 8760. The curve is shown in Figure 3.6.
4. Polynomial regression was performed on the sorted price curve, resulting in a fifth-degree polynomial function. This function is displayed in Figure 3.6 and Equation (3.11).
5. The water values are then found using the previously calculated h_{max} as input in Equation (3.11). The water values range from 12.59 €/MWh to 17.39 €/MWh, seen in Table 3.2.

$$-2.33 \cdot 10^{-17} \cdot x^5 + 5.82 \cdot 10^{-13} \cdot x^4 - 5.57 \cdot 10^{-9} \cdot x^3 + 2.52 \cdot 10^{-5} \cdot x^2 - 5.43 \cdot 10^{-2} \cdot x + 59.48 \tag{3.11}$$

After all the water values are obtained according to the description above, they are ready to be used in SHOP. SHOP has different methods for handling water value inputs, both

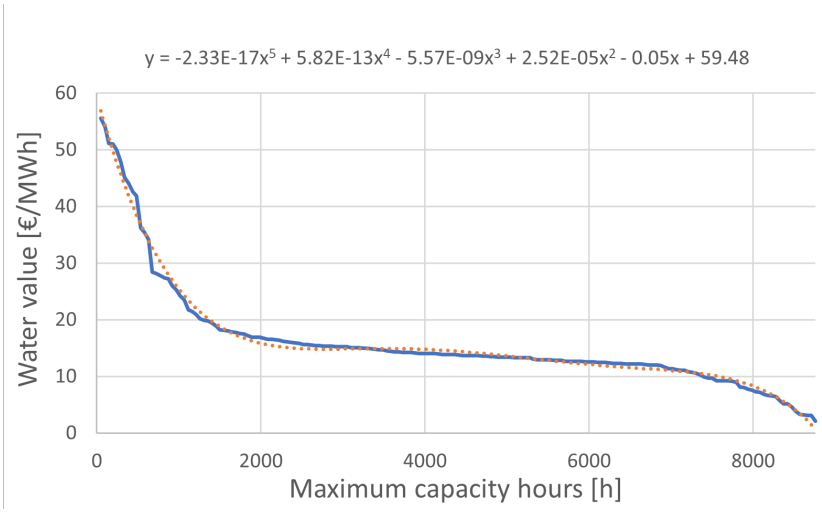

Figure 3.6: *Sorted electricity price curve for January 2022 to June 2022, along an x-axis ranging from 0 to 8760. The dotted line is a polynomial trend line.*

Table 3.2: *Water values calculated with Capacity Factor Method.*

Plant	Node	Water Value [€/ MWh]
Offervatn	Adamselv	17.39
Adamselv	Adamselv	14.82
Alta	Alta	13.74
Dividalen	Dividalen	13.41
Goulasjohka	Goulasjohka	14.67
Lassajavri	Kvaenangen	14.19
Smaavatna	Kvaenangen	14.27
Kvaenangsbotn	Kvaenangen	14.92
NedrePorsa	NedrePorsa	14.73
Skibotn	Skibotn	12.59

for dependent and independent water values. As the values in Table 3.2 are calculated with the Capacity Factor Method, they are independent, and thus incite the use of the *energy_value_input* attribute. This attribute acts like an input for local water values in SHOP, and by using this value for each reservoir, SHOP is able to calculate global water values in $\frac{€}{Mm^3}$. The global water values are calculated by summing up the local water values (in $\frac{€}{Mm^3}$) from the bottom of the watercourse and up, and thus achieving some level of dependent water values.

3.3.5 Load Demand

Consumption data for NO4 is available at Nord Pool [21]. The total consumption is calculated as consumption minus generation, plus imports minus exports. The data is provided with an hourly time frame for the whole price area, and internal flows and demand within the area are not given. Figure 3.7 illustrates the overall production and energy consumption from the 1st to the 8th of January 2022 in NO4. Given the high amount of hydropower in the Norwegian energy mix, the producer's flexibility becomes clear when analyzing Figure 3.7. The market price influences the amount of power produced and exported as long as the electricity demand is met. The nodal prices in the system are the same within the same price area. The only factor determining which hydropower unit produces electricity is the water value of each reservoir.

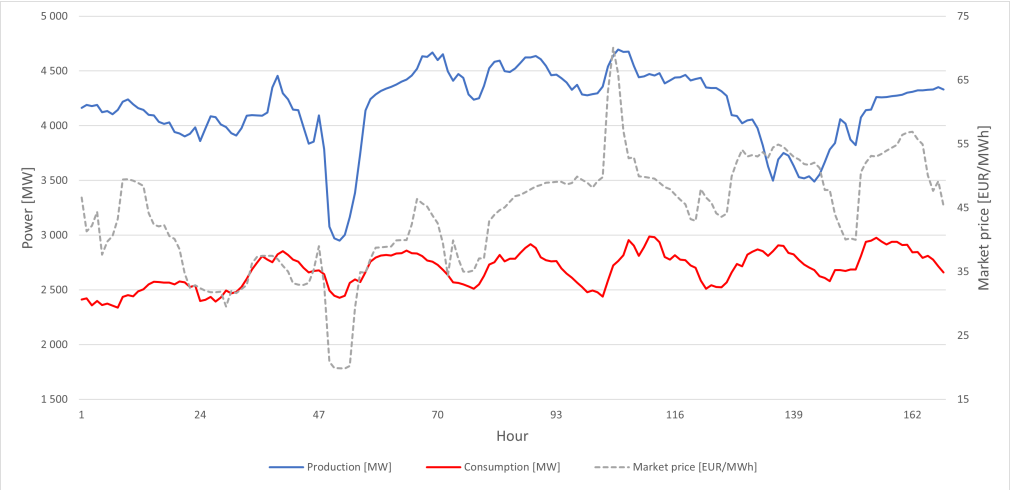

Figure 3.7: *Production (blue) and consumption (red) for NO4 in the first week of 2022. Data obtained from Nord Pool.*

The NVE data set includes load data for individual buses, which were subsequently adjusted in proportion to the total consumption data between January 1st and January 8th, marked with red in Figure 3.7. In this way, an accurate representation of the load curve could be represented in the model.

3.3.6 Modeling of unrepresented hydro and wind power

Modeling this system poses a significant challenge due to the limited inclusion of power production facilities in the network model. The Statkraft data set contains only a subset of the available power production facilities in the price area. As a result, the power generated from the excluded power stations must be included in the input data, thereby excluding it from the optimization process. Various approaches can be considered to address this problem. One potential solution is to scale the consumption curve by a scalar factor to ensure the load is appropriate for the modelled power stations. As this solution had the potential to produce an unrealistic power flow distribution, an alternative approach was pursued.

Historical wind power production data is available at Ref. [47]. As the data contains production history for individual power plants, the power production can be allocated to respective nodes in the NO4 model. Wind power functionality is currently not available in SHOP, and due to this, an alternative modeling approach was applied. By modeling the wind power plants as low volume hydropower reservoirs with an overflow option and a lossless generator, the wind power production can be emulated by utilizing the inflow of the reservoir. By approximating the density of water ρ to be 1000 $\frac{kg}{m^3}$ and the gravitational constant G to be 10 $\frac{m}{s^2}$, the correlation between inflow and power output can be seen in Equation (3.12). Using $h = 100$ m gives a 1:1 ratio between inflow x $[\frac{m^3}{s}]$ and power output P $[MW]$. [51].

$$\rho G h \cdot x = P \tag{3.12}$$

$$[\frac{kg}{m^3}] \cdot [\frac{m}{s^2}] \cdot [m] \cdot [\frac{m^3}{s}] = [\frac{kg \cdot m^2}{s^3}] = [W] \tag{3.13}$$

The implementation of this concept in SHOP involved the creation of reservoirs characterized by negligible volume and a 100 m difference in elevation between the inlet and outlet. These reservoirs were modeled with overflow gates and a lossless penstock leading to the downstream plant, as shown in Figure 3.8. The turbine and generator

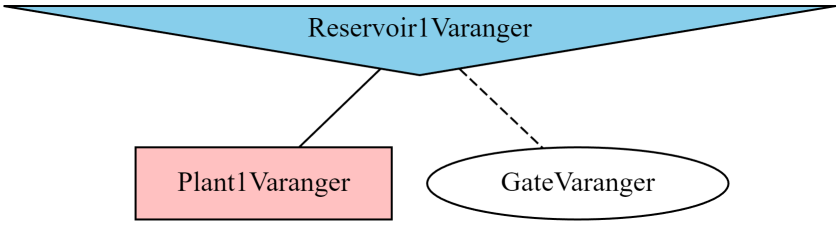

Figure 3.8: *Wind power plant modelled as hydropower*

efficiency were set at an optimal 100%, while both the water value and overflow cost were deliberately established at 0 to emulate the characteristics of unregulated renewable power. The production data obtained from each individual wind power plant was subsequently employed as inflow data for these reservoirs, enabling the plant to utilize the available power whenever necessary. Conversely, in cases where the power demand is not required, the reservoir automatically transitions into an overflow state. In practise, the wind power is modelled as a run-of-the-river power station with exceptionally high variability in water flow. One of these minuscule reservoir models is shown in Figure 3.8.

To model the unrepresented hydropower, a similar approach was employed. The same near-zero volume reservoirs were created and placed at their appropriate nodes within the NO4 model. However, due to the lack of publicly available production data for individual hydropower plants, an alternate approach had to be utilized to model the inflow. This problem was solved by using a similar solution strategy as the one used for demand modeling in Section 3.3.5. Power plant data from [46] was utilized to scale the NO4 production curve depicted in Figure 3.7. By using these scaled curves as inflow to the hypothetical reservoirs, the representation of hydropower production from the unmodeled plants was achieved. The utilization of the minuscule reservoir strategy serves a specific purpose: to prevent *power excess* in the simulation. By modeling the power production from unrepresented wind and hydro in this manner, the simulation ensures that production ceases when power becomes redundant. This approach enables a more precise representation of the net power at each node, thus allowing for power flow analysis.

3.4 PTDF module

Section 3.2 describes the constraints used in a typical STHS optimization problem. As one of the main focus areas of this thesis is to investigate the influence of including grid

limitations in hydropower scheduling, Equation (3.9) is of particular interest.

$$-F_{ij}^{MAX} \leq \sum_{bus=1}^{n} a_{ij,bus} \cdot P_{bus} \leq F_{ij}^{MAX} \tag{3.9}$$

By assuming DC power flow, the *Power Transfer Distribution Factors* $a_{ij,bus}$ can express power flow constraints on a transmission line between sending bus i and receiving bus j. In SHOP, PTDF data must be entered manually or imported from an external source. This section will elaborate on the PTDF module that was designed in Python to generate and export PTDF data.

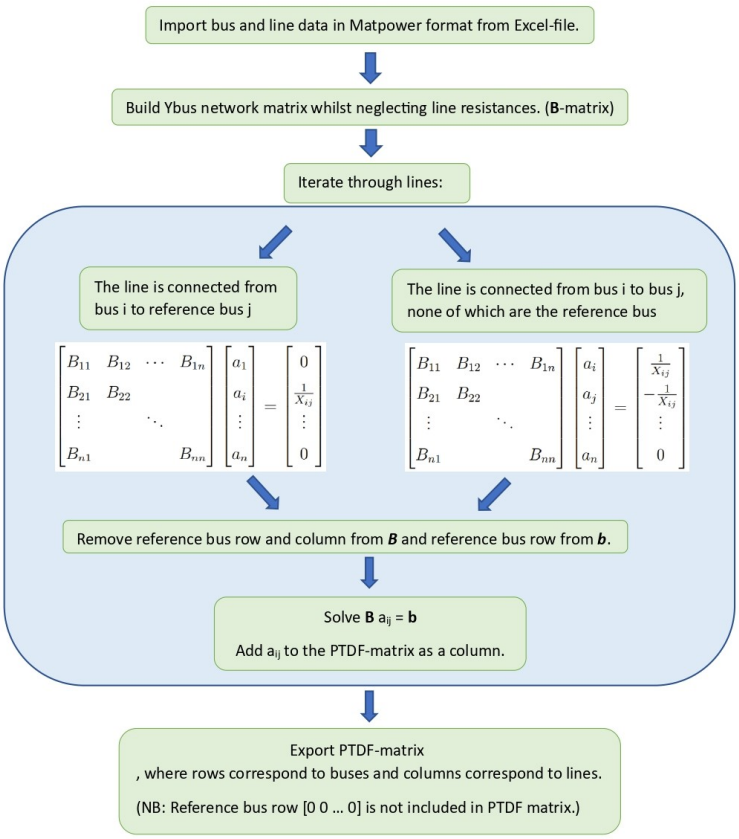

Figure 3.9: *Flowchart describing the PTDF module that was created to generate and export PTDF data.*

Figure 3.9 shows the flowchart for the Python module, where the first step is to import network data from an Excel file. The data is structured in the MATPOWER [52] format, widely used for power system analysis. Since PTDF calculations are independent of power injections and power flows through the system [32, 33], much of the information in the Excel file is redundant. The information needed is: System topology, line reactance,

and bus classification (identifying the designated reference bus). Since PTDF calculation is based on the DCPF assumptions, the generated Ybus bus is only dependent on line reactances, and the Ybus is hence referenced as matrix $\boldsymbol{B}$. After establishing the $\boldsymbol{B}$-matrix, the next step is to iterate through all the lines to determine the vector $\boldsymbol{b}$ from Equation (3.14).

$$\boldsymbol{B}a_{ij} = \boldsymbol{b} \tag{3.14}$$

There are two possibilities for each line: a) one of the lines is the reference bus, and b) none of the lines is the reference bus. For each scenario, the $\boldsymbol{b}$-vector is determined according to Section 2.3.1. Before solving for a_{ij} in Equation (3.14), the rows and columns related to the reference bus are removed from $\boldsymbol{B}$ and the reference bus row from vector $\boldsymbol{b}$. After solving for a_{ij} for each line, this vector now contains that line's *Power Transfer Distribution Factors*. The a_{ij} vectors are then combined to form the PTDF matrix for the entire system, where rows correspond to buses and columns correspond to lines. Note that the row corresponding to the reference bus is not calculated in this procedure. Since the reference bus is also acting as a balancing bus, a change in injection at this bus will not affect the line flows, and the PTDF vector for the reference bus is thus only composed of zeros. Equation (3.15) shows the structure of the PTDF matrix.

$$PTDF = \begin{bmatrix} a_{line1,bus1} & a_{line2,bus1} & \cdots & a_{lineM,bus1} \\ a_{line1,bus2} & a_{line2,bus2} & & \\ \vdots & & \ddots & \\ a_{line1,busN} & & & a_{lineM,busN} \end{bmatrix} \tag{3.15}$$

4 Results

The base case demonstrates the system behavior with one specified market, defining all internal grid limitations and *Power Transfer Distribution Factors* (PTDF). Subsequently, a contingency case is introduced, involving a line outage between buses 3 and 5, as described in Section 3.1.2. Lastly, a reduced model is introduced to show the example of a key attribute of PTDFs by targeting a smaller area within the original model. Appendix B provides the line utilization in each of the three cases.

4.1 Case 1: Base case

As seen in Figure 4.1, the production units at busbar Alta are the primary contributors to hydropower generation. With low water value, high demand, and low start-up costs, these units are valuable for meeting the base demand. The reservoir also has a more significant margin in volume before reaching the lowest regulation level. In contrast, the Skibotn reservoir, with a lower water value, provides less production from its units. The input data indicates a slightly higher main loss factor for the main tunnel at Skibotn. Additionally, the regulation levels at Skibotn have a smaller range. In conclusion, SHOP optimizes based on several economic parameters before deciding on a final scheduling scheme.

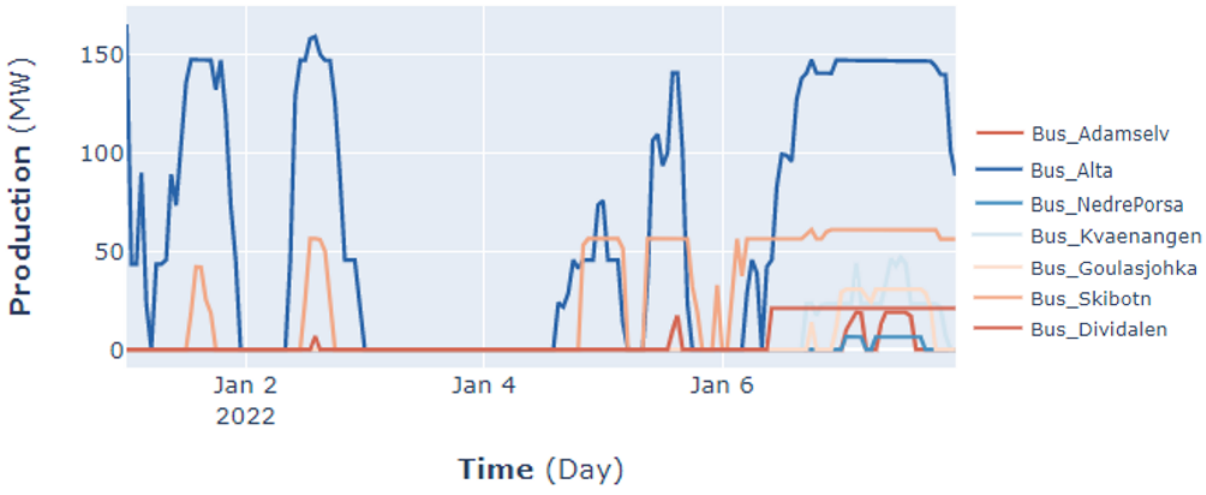

Figure 4.1: *Hydropower production from each bus, excluding wind power production.*

In SHOP, there are multiple ways to display the optimization objective value. Upon running the optimization process, two log files are automatically generated: "cplex.log"

and "shop_messages.log". The "cplex.log" file provides the actual solution values of the optimization problem, giving a comprehensive overview of the results. On the other hand, the "shop_messages.log" file offers a condensed representation by showcasing a selection of values derived from the solution. This log file aims to facilitate a better understanding of the solution and its implications. The importance of the disparity in values in these two files will be discussed when presenting the results for Case 2.

Table 4.1: *Objective values for Case 1*

Log file	Objective value
cplex.log	-9934902.020337
shop_messages.log	-9921589.48

4.2 Case 2: Line outage

The comparison between nearby lines in the outage scenario is depicted in Figure 4.2b, whereas the resulting flow in the reduced case is shown in Figure 4.2a. Specifically, the three lines from nodes 2-3, 3-5, and 4-5 are considered. In Figure 4.2b, line 3-5 is disconnected, resulting in zero flow. The outage only affects nearby lines, while the rest of the system maintains its existing flows. Lines 2-3 and 4-5 now accommodate the previous flow on 3-5. From the PTDFs in Appendix B, this network section in the outage case exhibits a radial structure. The PTDFs are then either 0 or -1 for the lines in this example.

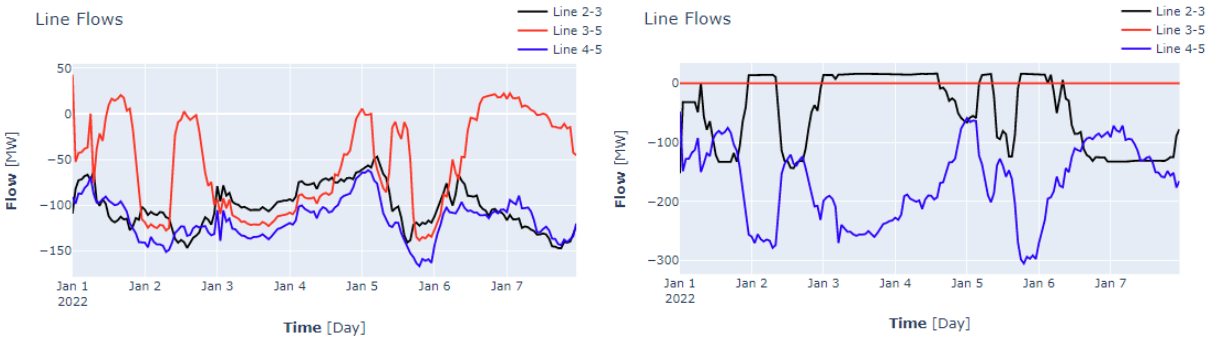

(a) *Line flow on nearby lines in reduced scenario.*

(b) *Line flows on nearby lines close to outage scenario.*

Figure 4.2: *Comparison of lines flows based on topology in Figure 3.3.*

Table 4.2 presents the two variations of the resulting objective value for Case 2. Upon comparing the objective value in the "shop_messages.log" with the one from Case 1, a minor discrepancy of 600 NOK is observed. At first glance, this variance might appear perplexing, considering the fact that a greater absolute value is an indication of a superior solution. However, when comparing the "cplex.log" values, the absolute value for Case 1 is greater than for Case 2, indicating that Case 1 is indeed the superior solution. This contradiction is due to the fact that the power flow functionality of SHOP is still in its early stages of implementation, resulting in certain factors like *load penalties* being absent from the "shop_messages.log" file. However, upon comparing the "cplex.log" values, it becomes apparent that the 600 NOK discrepancy is outweighed by factors that are not accounted for in the "shop_messages.log" output. It is worth mentioning that since no lines are congested in either of the cases, there is still little difference in the overall objective values.

Table 4.2: *Objective values for Case 2*

Log file	Objective value
cplex.log	-9934902.014894
shop_messages.log	-9922189.48

4.3 Case 3: Reduced model

Like the base case, the production units meet the base demand (Figure 4.3a). Coordinated with the wind power production, no additional hydropower units are required until the final day. Since none of the transmission lines are congested, the energy price remains the same at all nodes, as seen in Figure 4.3b. Figure 4.3a and 4.3b illustrate a strong correlation between hydropower production and the energy price over the 7-day period. It is important to note that in a real-world scenario with a nodal pricing scheme, congestion would result in different energy prices. Furthermore, the topology in Figure 3.3 restricts the extensive need for hydropower production within the reduced area.

In Table 4.3, the PTDFs for three different lines are compared between the base case (14 buses) and Case 3 (6 buses). Reducing the system is advantageous when focusing on

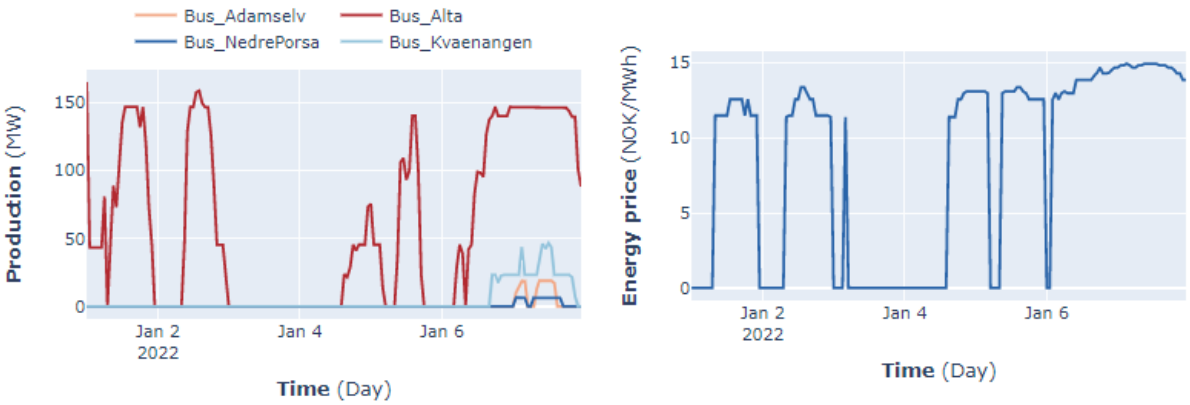

(a) *Hydropower production (MW).* **(b)** *Dual value of energy price ($\frac{NOK}{MWh}$).*

Figure 4.3: *Hydropower production and energy price in reduced case*

specific areas, such as contingency analysis. The table reveals that the PTDFs within the equivalent zone are similar, resulting in identical line flows across all lines.

Table 4.3: *PTDFs for selected lines between bus 2-4, 3-5 and 4-5. In Case 2, line 3-5 is disconnected.*

Lines	2-4		3-5		4-5	
Bus	Base case	Case 3	Base case	Case 3	Base case	Case 3
1	0	0	0	0	0	0
2	0	0	0	0	0	0
3	-0.3189	-0.3189	-0.31885	-0.3189	-0.3189	-0.3189
4	-0.7303	-0.7303	-0.2697	-0.2697	0.2697	0.2697
5	-0.4825	-0.4825	-0.5175	-0.5175	-0.4825	-0.4825
6	-0.4825	-0.4825	-0.5175	-0.5175	-0.4825	-0.4825
7	-0.4825	-	-0.5175	-	-0.4825	-
8	-0.4825	-	-0.5175	-	-0.4825	-
9	-0.4825	-	-0.5175	-	-0.4825	-
10	-0.4825	-	-0.5175	-	-0.4825	-
11	-0.4825	-	-0.5175	-	-0.4825	-
12	-0.4825	-	-0.5175	-	-0.4825	-
13	-0.4825	-	-0.5175	-	-0.4825	-
14	0	0	0	0	0	-

5 Discussion

This section discusses the case studies conducted in SHOP to test the functionality of *Power Transfer Distribution Factors* (PTDF) in *Short-Term Hydro Scheduling* STHS. It also discusses the current status and potential applications of PTDF modeling in SHOP. Additionally, possible future market clearing strategies are explored.

5.1 Case studies

The analysis of STHS is conducted through a comparative study of three cases. The base case, which forms the foundation of the study, examines a normal load scenario that represents the current power situation in NO4. In this scenario, the power demand is considerably lower than the capacity that could be transmitted over the line. A realistic depiction of the existing power conditions is therefore provided. The PTDF modeling utilizes nodal pricing, where electricity prices reflect each physical constraint of the transmission grid. As the PTDFs effectively distribute power in the base case, congestion behavior is eliminated, resulting in an equal market price for all nodes.

Using zonal PTDF matrices can assist *Transmission System Operators* (TSO) in relieving congestion and reducing the reliance on counter-trading. This approach can benefit the TSO during the pre-market coupling phase, which serves as the preparation stage for day-ahead modeling. Instead of modeling the entire grid, which can be computationally challenging, a possible approach is to focus on modeling the critical branches most impacted during contingency scenarios [42]. In addition, implementing a counter-trading scheme could serve as a backup alternative to this approach. It becomes particularly advantageous in outage scenarios, as illustrated in Case 2. Only neighboring lines redistribute the power flow previously transmitted through the disconnected line, effectively relieving this load. Additional testing is recommended for high-demand and stressed systems scenarios to further assess performance and potential improvements.

5.2 PTDF applications in SHOP

The transmission system modeling and power flow functionalities in SHOP are currently in the early stages of development. It is therefore crucial to emphasize the future

potential of this functionality. The three optimization cases discussed in this thesis highlight some benefits of PTDF in a *Short-Term Hydro Scheduling* tool like SHOP. The PTDF factors for these cases were generated using the developed PTDF module. Apart from generating distribution factors, this module demonstrates its capability as a standalone tool in generating optimization constraints for the STHS problem within SHOP. It provides the necessary flexibility to generate and import constraints, opening up opportunities for further development and expanding its functionality and usefulness. This chapter not only delves into the potential benefits and challenges associated with incorporating PTDF and similar methodologies, but also explores the untapped potential of the PTDF module itself.

One of the reasons why including grid constraints in STHS is essential is to be better suited for the future power system. With the anticipated rise in electrical load demand, optimizing the utilization of the transmission grid and available water resources becomes imperative. The projected increase in load has the potential to strain the power system, exerting pressure on transmission lines that could approach their transmission capacity limits. Any single or multiple line faults could lead to power redistribution onto neighboring transmission lines, thereby leading to additional faults in the system [38].

One possible approach to address the challenges discussed above is the combination of LODF (Line Outage Distribution Factors) with Benders Decomposition, as detailed in Section 2.3. Benders Decomposition involves dividing the optimization problem into a master problem and subproblems. By analyzing the solutions of the subproblems and incorporating them into the master problem, security constraints can be effectively considered without significantly increasing the complexity of the original optimization problem. Integrating a Benders Decomposition module could either be an addition to the existing PTDF module or a standalone one. Given the inherent complexity of the SHOP optimization, implementing Benders Decomposition would likely need to be performed externally. For instance, a Benders master problem could be constructed, resembling the objective function and constraints of the optimization problem in Case 1. An optimal solution with a specific set of solution variables would be achieved by iterating through the subproblems. These variables could then add constraints to the SHOP optimization,

thus enabling a security-constrained optimization. The constraints would typically be restrictions on generator dispatch and line flows. A similar approach is found in Ref. [53], where Lagrangian relaxation and Benders Decomposition are combined to address complex optimization problems.

Case 3 illustrated the potential of modeling a smaller area within a larger system to simplify the simulation complexity. However, this approach heavily depends on accurately approximating the power flow entering and leaving the smaller system. Considering that the conventional usage of SHOP involves hydropower producers exclusively modeling their hydropower plants without considering the broader grid, this presents a notable challenge. Furthermore, Figure 4.2 demonstrates the significant fluctuations in line flows over a week. This implies that while the average flow pattern in an area may be known, predicting the hourly variations is challenging. With the introduction of *Flow-Based Market Coupling* (FBMC), as discussed in the next chapter, the TSO will have better insight into real-time and future flow in the system [28]. However, if this valuable information were accessible to all hydropower producers, it could potentially create opportunities for market exploitation. Because of this reason, there needs to be implemented a system to handle the intricacies behind profit management. However, since this topic primarily involves a shift in market infrastructure, it will be further explored and addressed in Section 5.3.

To accurately model the future power system in SHOP, it is necessary to include branch resistances for contingency events in sub-transmission and transmission networks with low X/R-ratio (reactance/resistance). This model maintains the efficiency of the DC power flow method, ensuring linearity and fast matrix inversion lemma for branch outages. Ref. [54] suggests two methods for implementing PTDFs. The first method is a generalized linear PTDF approach that includes the branch resistances. The second method utilizes the sparse matrix technique for characteristic contingency cases, such as injection changes and branch outages. By applying this model in SHOP, it can be used for power system analysis, planning, and operation under various scenarios. The future power system faces challenges due to increasing variability in load demand, particularly with the addition of new industries connected to lower voltage levels. Hence,

this application becomes valuable in SHOP for efficiently distributing available power.

To summarize, the development of network modeling and power flow functionalities in SHOP shows promising potential for future applications. The use of PTDFs in optimization cases demonstrates the benefits of PTDFs in STHS. Addressing grid constraints is crucial to optimize the utilization of the future power system and water resources. Modeling smaller areas within the system can simplify simulations, but an accurate approximation of power flows is essential. Including contingency analysis and considering branch resistances for congestion scenarios are recommended improvements. Incorporating these advancements in SHOP can enhance power system analysis and operation.

5.3 PTDF and reflections on future market clearing strategies

The preceding section has discussed the various applications and benefits of incorporating *Power Transfer Distribution Factors* (PTDF) into an STHS program like SHOP. The insight gained from the STHS domain may also be useful for discussing the implementation of PTDF in clearing the electricity market. This topic has lacked discussion over the years because there has been no need for its implementation in the Nordic electricity market. However, recent developments in the Nordic electricity market, characterized by significant growth in price disparities, have brought it to the forefront of relevance. The planned implementation of FBMC has further intensified the interest in the matter.

Although the current debate in the Nordic electricity market revolves around the choice between the ATC and FBMC approaches, discussing more comprehensible examples could be valuable. Because of this, three suggested levels of PTDF implementation will be discussed to understand the different impacts PTDF can have. The examinations of these three levels seek to assess and distinguish the varied effects of PTDF on market outcomes and system operation.

Node pricing: The complete utilization of PTDF will lead to the establishment of a nodal pricing system. This enables the market clearing algorithm to have comprehensive visibility into power flow and congestion risks within the system. With this system, producers in advantageous positions will have the ability to set higher prices for their

electricity. This opportunity for market exploitation induces the need for a regulating authority. In the US, where nodal pricing has been used for many years, the regulating body FERC (*Federal Energy Regulatory Commission*) was created specifically to prevent such exploitative practices [55]. There are several reasons why this pricing system has not been favorable in the Nordic energy system. One key factor is the successful history of cross-border energy exchange within the Nordic countries, which has been facilitated by the existing pricing system. Introducing nodal pricing would significantly increase the complexity of this well-functioning dynamic, potentially disrupting the efficient cross-border flow of energy.

Sub-system representation: Much like in Case 3, congestion-prone zones can be accounted for in the market clearing using PTDF. This approach is the basis of the FBMC methodology. While flow-based market coupling offers improved utilization of the existing grid, there are several important considerations to bear in mind. A fundamental premise of this approach is the requirement for the TSO to possess accurate real-time information about the system's conditions. This necessitates a higher level of cooperation between market participants and system operators to ensure the availability of reliable data. Moreover, the exchange and storage of such data introduce a potential cybersecurity threat, as unauthorized access or manipulation of this information could provide significant market advantages or be used with malicious intent. In Norway, government agencies NVE and Statnett have been trusted to secure fair competition in the electricity market. With the introduction of a FBMC-related market algorithm, the need for monitoring and regulation is even greater, and the regulating authorities will have an important role in mitigating the associated risks.

Multi-period consideration: An alternative approach to implementing PTDF in a nodal pricing system is using a market algorithm that considers multiple time periods simultaneously. This approach could utilize PTDFs to identify congestion during the market-clearing process, so that producers affected by a bottleneck are either up or downregulated. Instead of getting a nodal price for these producers, a compensation system would need to be established to ensure that down-regulated producers in high-price hours are adequately compensated for their financial losses. The same would

apply to producers who are up-regulated during low-price time intervals. Overall, this would result in smoother prices and better utilization of the transmission grid. However, several challenges exist in implementing this approach in the Nordic energy market. One of the primary challenges is the complexity of introducing a compensation system, which, if not managed effectively, could result in winners and losers at the local level. Also, implementing this approach while upholding the high standards of transparency typically observed in Norway would present considerable obstacles.

The above analysis highlights the challenges associated with different levels of PTDF implementation in the market clearing algorithm. However, due to more volatility and disparity in electricity prices, new methods for congestion mitigation are needed. In this regard, considering the trade-offs, it can be argued that the FBMC approach is the most favorable option for the Nordic electricity market. It balances between improved grid utilization and the need for reliable data while building upon existing regulatory frameworks. Ultimately, the choice of PTDF implementation should consider the specific characteristics and priorities of the electricity market.

Network modeling and market considerations play crucial roles in the context of incorporating FBMC in future power system scenarios. Managing market boundaries is an important aspect to consider in network modeling, which has the potential to enhance social welfare and minimize grid investments. The goal of incorporating FBMC during the second quarter of 2023 in the Nordics [28], aims to address this issue. The northern part of Norway as one price zone is not ideal, and FBMC could simplify the handling of market boundaries. However, market power within the price zone remains challenging, as power producers with regulatory capabilities could exploit their position to manipulate prices. If the margin within the price area is narrow and individual producers significantly impact available capacity, it could pose a problem. The government continuously monitors such situations to ensure a justified power market. Therefore, splitting price areas should be pursued only if there is enough competition within each new zone.

In addition to managing market boundaries, the incorporation of other concepts in FBMC is crucial for effectively analyzing power systems, such as Generation Shift Keys (GSKs) and Critical Branches (CBs). Ref. [44] discussed how these are used in the pre-market

coupling, while Ref. [42] explored possible implications for traders. GSK is a factor describing the most probable change in net injection at a node relative to a change in net position of the zone that it belongs to. The GSKs and nodal PTDF matrices are used to calculate the zonal PTDF matrices for each price area during market clearing. The CBs impose flow restrictions for transmission lines significantly impacted by cross-border trading [44]. The TSO could then decide on the CBs based on the PTDF matrix in the pre-market phase. A difficulty for the TSO is identifying the correct CBs before the market clearing. Incorporating these factors, along with PTDFs, into future power system scenarios can provide valuable insights into analyzing internal grid limitations within SHOP. This approach can effectively partition large price areas into smaller, equivalent zones using FBMC, offering potential benefits in terms of market efficiency and addressing congestion challenges.

5.4 Critical reflection

The accuracy of the optimization process is dependent on the quality of the input data. This data was obtained from openly available sources such as NVE Atlas, NVE Sildre, and Statnett reports. However, it should be noted that some of the data may be outdated or incorrect. In addition, missing line data and reliance on assumptions when estimating reactance can impact the weighting of the PTDFs and potentially lead to under- or overestimation of line capacity. These factors should be carefully considered to ensure reliable and accurate results in the optimization. This chapter will discuss the eligibility of the optimization and focus on parameters that affect the calculation of the PTDFs. While the case studies in this thesis aimed to closely resemble the current power system in NO4, the primary focus was not on analyzing the optimization results regarding grid utilization and system performance. Instead, the main objective was to exemplify and emphasize the features of PTDF. Consequently, the most significant parameters to discuss in this chapter are those that directly impact the calculation of PTDF.

One parameter that directly impacts the PTDF calculation is the line reactance. These values were sourced from the classified NVE file, which provides accurate information for each line in the system. However, it is worth noting that certain lines were missing from the file, requiring estimations to be made for those particular cases. To achieve

correct results using PTDF, the accuracy of the system topology and line reactances is of utter importance. The impact resistance has on line loss was not addressed in this study. However, it is possible to model this using a linear loss factor in SHOP, which is proportional to the absolute value of the line flow, as described in Ref. [37]. The line losses in the DC power flow solution are divided equally by each line's nodes. According to this study, the losses significantly impacted the total operational costs, and computational time was only modestly affected by increased accuracy in loss estimation. Based on Ref. [56], an X/R ratio > 2 results in an active power error of less than 5%. Neglecting resistance in this study may overestimate line flows, particularly in the 132 kV network.

Since PTDF is primarily employed to compute line flows by considering the power balance at each node, having accurate knowledge about load distribution within the system is crucial. Obtaining precise information on real-time load distribution poses a challenge, particularly for individual producers who do not have direct access to such data. As the case studies in this thesis were deterministic, historical data on load consumption for NO4 was available at Nordpool. However, even with this information, there is no available information about the load distribution within the price zone. Consequently, assumptions had to be made, such as distributing the load based on restricted data from NVE and scaling each load to match the overall load curve. The information dependency of PTDF poses a significant challenge when implementing it in *Short-Term Hydro Scheduling*. This issue becomes particularly pronounced in the context of larger hydropower producers with multiple plants spread across the country, as they may have access to more data compared to smaller producers. To address this concern, one possible solution is for the Transmission System Operators to establish a system that ensures equitable access to data for all producers.

The full AC power flow is the most accurate approach, as the DC method used for PTDFs is based on approximations. This includes ignoring the reactive power balance equations, assuming all voltage magnitudes are equal to one per unit, and ignoring line losses [40]. The X/R line ratio condition can also be difficult to guarantee. Ref. [56] investigated X and R values for the Belgian high voltage grid. The results showed that

X/R ratios varied between 0.8 (70 kV) and 12.5 (380 kV). The X/R ratio should be high enough, otherwise, the assumption of negligible resistance is violated. Here, a proposed border value was set at X/R = 4. For this thesis, the X/R ratios ranged from 2.75 (132 kV) for the minimum line ratio to 13.55 (420 kV) for the maximum. This highlights a significant variability in the system's impedance characteristics across voltage levels.

There are additional input parameters that do not directly impact the calculation of PTDF. The discussion surrounding these parameters can give valuable insights for a better understanding of the optimization results. Among the input data, the water values emerge as the most questionable. Due to their confidential nature, significant assumptions had to be made, resulting in a departure from realistic values. This discrepancy directly impacts the distribution dispatch among hydro plants within the system, and thus the line flows. Another parameter of relatively lesser significance is precipitation, which holds greater relevance for medium- and long-term scheduling. Lastly, the treatment of unmodelled hydropower plants in the optimization raises concerns. These plants were merely treated as wind power plants with a production curve scaled to the overall production curve of NO4, with the rated power of the plant as a basis. Ideally, a SHOP model should be implemented for all hydropower plants in the system, ensuring an accurate representation of their unique characteristics.

6 Conclusion

The objective of this thesis was to investigate the implementation and utilization of *Power Transfer Distribution Factors* (PTDF) in *Short-Term Hydro Scheduling* (STHS). The problem definition stemmed from the projected increase in load demand and the introduction of Flow-Based Market Coupling in the Nordic Electricity Market. To address this problem, a module was developed to generate and import PTDF factors into the STHS tool SHOP. Utilizing transmission system modeling, a novel feature within SHOP, the PTDF factors were generated and applied to three optimization cases. These examples were based on a comprehensive system model of NO4 specifically developed for this thesis.

Case 1 showcased how PTDF factors are used to generate optimization constraints within the SHOP optimization core. Additionally, these factors were employed to visualize the resulting line flows in the system. Case 2 focused on generating PTDFs for a line outage scenario, revealing how the power flow is efficiently redistributed away from the faulted line through the optimization process. Case 3 presented an example of generating PTDF for a smaller section within a larger area, emphasizing the importance of precise data regarding power flow into and out of the smaller area to obtain accurate results.

The discussion on the developed PTDF module concluded with recognizing the advantages of having a dedicated module capable of generating constraints for the optimization problem. In addition to PTDF, the module was also considered for incorporating contingency analysis and congestion management techniques. The insights derived from the conducted case studies in SHOP were utilized to examine different levels of PTDF implementation in the electricity market clearing process. The discussion encompassed various pricing approaches, including nodal pricing and zonal pricing with FBMC. The key conclusion drawn was that incorporating grid constraints into the market clearing algorithm introduces complexities related to market manipulation and unfair market positions. Addressing these challenges will require enhanced collaboration between Transmission System Operators and power producers.

To conclude, utilizing *Power Transfer Distribution Factors* in *Short-Term Hydro Scheduling* and as a market clearing mechanism exhibits significant promise. Nevertheless, un-

locking this potential hinges on establishing a robust system that guarantees a just and equitable power market.

6.1 Further work

SINTEF ER should prioritize further research on the implementation of power flow analysis in SHOP. Currently, hydropower producers in SHOP typically model only their own plants and infrastructure, but there is a need to develop a system for considering the rest of the power system and grid. Although the power flow functionality exists in SHOP, it has not been integrated into the conventional use of the tool.

The developed PTDF module holds significant potential for expanding its functionality, particularly with the inclusion of Benders Decomposition for contingency analysis and the implementation of a system for PTDF equivalents. These additions can greatly enhance the usefulness of the module in STHS.

The implementation of Flow-Based Market Coupling will be an intriguing aspect to observe going forward. While incorporating grid constraints into the market clearing algorithm is a challenging endeavor, the primary concern lies in establishing a system that guarantees fair competition, rather than the technical implementation itself. The radial structure of the NO4 grid, in particular, increases its vulnerability to market exploitation.

Bibliography

[1] Jiehong Kong, Hans Ivar Skjelbred, and Olav Bjarte Fosso. "An overview on formulations and optimization methods for the unit-based short-term hydro scheduling problem". In: *Electric Power Systems Research* 178.August 2019 (2020), p. 14. ISSN: 03787796. DOI: 10.1016/j.epsr.2019.106027.

[2] Statnett. *Annual report 2021 The green change of pace*. Tech. rep. 2021. URL: https://www.statnett.no/en/about-statnett/investor-relations/annual-and-semi-annual-reports/.

[3] Statnett. *Long-term Market Analysis 2020-2050 (Update Spring 2021)*. Tech. rep. 2021. URL: https://www.statnett.no/globalassets/for-aktorer-i-kraftsystemet/planer-og-analyser/lma/lma-update-2021.pdf.

[4] Statnett. *1st halfyear 2022*. Tech. rep., pp. 1–24. URL: https://www.statnett.no/en/about-statnett/investor-relations/annual-and-semi-annual-reports/.

[5] Norges vassdrags- og energidirektorat (NVE). *Norsk og nordisk effektbalanse fram mot 2030*. Tech. rep. 20. 2022. URL: https://publikasjoner.nve.no/rapport/2022/rapport2022_20.pdf.

[6] Fabrício Y.K. Takigawa et al. "Solving the hydrothermal scheduling problem considering network constraints". In: *Electric Power Systems Research* 88 (2012), pp. 89–97. ISSN: 03787796. DOI: 10.1016/j.epsr.2012.02.005.

[7] Marius Eriksen and Mathias Espeland Trondal. "The Influence on Day-Ahead Trading Volumes by Including Power Flow Equations in The Planning Algorithm for Short-Term Hydropower in Congested Areas". In: *International Conference on the European Energy Market, EEM* 2022-Septe (2022). ISSN: 21654093. DOI: 10.1109/EEM54602.2022.9921169.

[8] Espen F. Bødal et al. "Coordination of hydro and wind power in a transmission constrained area using SDDP". In: *Proceedings - 2016 51st International Universities Power Engineering Conference, UPEC 2016* 2017-Janua (2016), pp. 1–6. DOI: 10.1109/UPEC.2016.8114017.

[9] Arild Helseth et al. "A model for optimal scheduling of hydro thermal systems including pumped-storage and wind power". In: *IET Generation, Transmission and*

Distribution 7.12 (2013), pp. 1426–1434. ISSN: 17518687. DOI: 10.1049/iet-gtd.2012.0639.

[10] Andreas Hovde Bo et al. "The impact of Flow-Based Market Coupling on the Nordic region". In: *International Conference on the European Energy Market, EEM* 2020-Septe (2020), pp. 1–6. ISSN: 21654093. DOI: 10.1109/EEM49802.2020.9221952.

[11] Viljar Stensaker Stave et al. "Optimal utilisation of grid capacity for connection of new renewable power plants in Norway". In: *SEST 2021 - 4th International Conference on Smart Energy Systems and Technologies* (2021). DOI: 10.1109/SEST50973.2021.9543304.

[12] Arild Helseth and Albert Cordeiro Geber de Melo. *Scheduling Toolchains in Hydro-Dominated Systems*. Tech. rep. Trondheim: SINTEF Energy Research, 2020, p. 74. URL: https://hdl.handle.net/11250/2672581.

[13] Sivert Forbord and Håkon Sølberg. *Optimal operation of hydropower considering grid constraints - Specialization Project*. Trondheim, 2022.

[14] Olav Bjarte Fosso. "Hydro scheduling with transmission transfer limitations in a liberalized power market". In: (2009). URL: https://www.researchgate.net/publication/306444891.

[15] Olav Bjarte Fosso and Michael Martin Belsnes. "Short-term hydro scheduling in a liberalized power system". In: *2004 International Conference on Power System Technology, POWERCON 2004*. Vol. 2. 2004, pp. 1321–1326. ISBN: 0780386108. DOI: 10.1109/icpst.2004.1460206.

[16] Stephen P. Boyd and Lieven Vandenberghe. *Convex optimization*. Cambridge University Press, 2004, p. 716. ISBN: 9780521833783.

[17] Hans Ivar Skjelbred, Jiehong Kong, and Olav Bjarte Fosso. "Dynamic incorporation of nonlinearity into MILP formulation for short-term hydro scheduling". In: *International Journal of Electrical Power & Energy Systems* 116 (Mar. 2020), p. 105530. ISSN: 0142-0615. DOI: 10.1016/J.IJEPES.2019.105530.

[18] Olav B Fosso. *ET6204 - Shortterm Hydro Power Production Scheduling*. Lecture slide. 2022.

[19] Gerard Doorman. "Course ELK15 Hydro Power Scheduling Professor Gerard L . Doorman Department of Electric Power Engineering NTNU Autumn 2009". In: *Power Engineering* (2009).

[20] Terje Gjengedal, Michael M. Belsnes, and Prof Olav B Fosso. "Methods for Short-term Generation Scheduling in Hydro Power Dominated Power Systems Methods for Short-term Generation Scheduling in Hydro Power". In: IEEE Xplore (2005).

[21] Nord Pool Group. "Nord Pool - Day-Ahead". In: *(Date accessed: 2023-04-24)* (). URL: https://www.nordpoolgroup.com/.

[22] Petr Spodniak, Kimmo Ollikka, and Samuli Honkapuro. "The impact of wind power and electricity demand on the relevance of different short-term electricity markets: The Nordic case". In: *Applied Energy* 283 (Feb. 2021). ISSN: 0306-2619. DOI: 10.1016/J.APENERGY.2020.116063.

[23] Statnett. "Tertiærreserver - mFRR". In: *(Date accessed: 2023-02-21))* (2018). URL: https://www.statnett.no/for-aktorer-i-kraftbransjen/systemansvaret/kraftmarkedet/reservemarkeder/tertiarreserver/.

[24] Mette Bjørndal, Kurt Jørnsten, and Virginie Pignon. "Congestion Management in the Nordic Power Market — Counter Purchases and Zonal Pricing". In: *Competition and Regulation in Network Industries* 4.3 (2003), pp. 271–292. ISSN: 1783-5917. DOI: 10.1177/178359170300400302.

[25] Mette Bjørndal and Kurt Jörnsten. "Benefits from coordinating congestion management-The Nordic power market". In: *Energy Policy* 35.3 (2007), pp. 1978–1991. ISSN: 03014215. DOI: 10.1016/j.enpol.2006.06.014.

[26] Statnett. "Nettutviklingsplan 2021 (Date accessed: 2023-03-03)". In: (2021). URL: https://www.statnett.no/for-aktorer-i-kraftbransjen/planer-og-analyser/nettutviklingsplanen/.

[27] Norges offentlige utredninger. "NOU 2022: 6". In: *(Date accessed: 2023-02-12)* (June 2022). URL: https://www.regjeringen.no/no/dokumenter/nou-2022-6/id2918464/.

[28] Statnett. "Kraftsystemet i Finnmark". In: *(Date accessed: 2023-03-14)* (2016), p. 206. URL: https://www.statnett.no/globalassets/for-aktorer-i-kraftsystemet/planer-og-analyser/kraftsystemet-i-finnmark.pdf.

[29] Statnett. "Kraftsystemet i Sør-Trøndelag og Nordmøre 2020-2030 Analyserapport". In: *(Date accessed: 2023-03-10)* (2020). URL: https://www.statnett.no/globalassets/for-aktorer-i-kraftsystemet/planer-og-analyser/

kraftsystemet-i-sor-trondelag-og-nordmore-2020-2030.-analyserapport-2017.pdf.

[30] Statnett. "Områdeplan Nord Nordre Nordland ," in: *(Date accessed: 2023-04-24)* September (2022), p. 13. URL: https://www.statnett.no/for-aktorer-i-kraftbransjen/planer-og-analyser/omradeplaner/.

[31] Olav Bjarte Fosso. "SHOP - Teoretisk gjennomgang (Presentasjon)". In: (2013), pp. 1–32.

[32] Gerald B. Sheble Allen J. Wood Bruce Wollenberg. *Power Generation, Operation and Control*. 2014, p. 658. ISBN: 9780471790556.

[33] Darko Šošić and Ivan Škokljev. "Features of Power Transfer Distribution Coefficients in power System Networks". In: *Infoteh-Jahorina* 13.November (2014), p. 86. URL: https://www.researchgate.net/publication/283087678.

[34] Prof Olav B Fosso. ""TET4575 - Kraftsystemer" - Distribution Factors & DC Optimal Power Flow". In: ().

[35] B Stott and O Alsac. "Fast Decoupled Load Flow". In: *IEEE Transactions on Power Apparatus and Systems* PAS-93.3 (1974), pp. 859–869. DOI: 10.1109/TPAS.1974.293985.

[36] William Ford. "Gaussian Elimination and the LU Decomposition". In: *Numerical Linear Algebra with Applications* (2015), pp. 205–239. DOI: 10.1016/B978-0-12-394435-1.00011-9.

[37] Arild Helseth. "A linear optimal power flow model considering nodal distribution of losses". In: *9th International Conference on the European Energy Market, EEM 12* 2 (2012). DOI: 10.1109/EEM.2012.6254717.

[38] Chong Suk Song et al. "Implementation of PTDFs and LODFs for Power System Security". In: *Journal of International Council on Electrical Engineering* 1.1 (Jan. 2011), pp. 49–53. DOI: 10.5370/jicee.2011.1.1.049.

[39] M Shahidehopour and Yong Fu. "Benders decomposition: applying Benders decomposition to power systems". In: *IEEE Power and Energy Magazine* 3.2 (2005), pp. 20–21. ISSN: 1558-4216. DOI: 10.1109/MPAE.2005.1405865.

[40] Xu Cheng and Thomas J. Overbye. "PTDF-based power system equivalents". In: *IEEE Transactions on Power Systems* 20.4 (Nov. 2005), pp. 1868–1876. ISSN: 08858950. DOI: 10.1109/TPWRS.2005.857013.

[41] Mahir Sarfati, Mohammad Reza Hesamzadeh, and Pär Holmberg. "Production efficiency of nodal and zonal pricing in imperfectly competitive electricity markets". In: *Energy Strategy Reviews* 24.August 2018 (2019), pp. 193–206. ISSN: 2211467X. DOI: 10.1016/j.esr.2019.02.004. URL: https://doi.org/10.1016/j.esr.2019.02.004.

[42] Tarjei Kristiansen. "The flow based market coupling arrangement in Europe: Implications for traders". In: *Energy Strategy Reviews* 27 (2020), p. 100444. ISSN: 2211467X. DOI: 10.1016/j.esr.2019.100444. URL: https://doi.org/10.1016/j.esr.2019.100444.

[43] Gerard L Doorman and Hossein Farahmand. "Flow-Based Market Coupling - TET4185 Blackboard notes." In: *NTNU Department of Electric Power Engineering* (2019), p. 23.

[44] Endre Bjørndal, Mette Bjørndal, and Hong Cai. "Flow-Based Market Coupling in the European Electricity Market - A Comparison of Efficiency and Feasibility". In: *Norwegian School of Economics* (2018). ISSN: 1500-4066.

[45] Hans Ivar Skjelbred. "Unit-based Short-term Hydro Scheduling in Competitive Electricity Markets". PhD thesis. 2019. ISBN: 978-82-326-4019-5.

[46] NVE. "Vannkraftdatabase - NVE". In: *(Date accessed: 2023-05-12))* (). URL: https://www.nve.no/energi/energisystem/vannkraft/vannkraftdatabase/.

[47] Norges vassdrags- og energidirektorat (NVE). "Data for utbygde vindkraftverk i Norge". In: *(Date accessed: 2023-05-13)* (2022). URL: https://www.nve.no/energi/energisystem/vindkraft/data-for-utbygde-vindkraftverk-i-norge/.

[48] NVE. "Kart | NVE Sildre". In: *(Date accessed: 2023-05-13)* (). URL: https://sildre.nve.no/.

[49] Muhammad Kamran. "Hydro energy". In: *Renewable Energy Conversion Systems* (Jan. 2021), pp. 193–219. DOI: 10.1016/B978-0-12-823538-6.00007-5.

[50] U. Aswathanarayana. "Hydropower". In: *Green Energy: Technology, Economics and Policy* (2010), pp. 39–43. DOI: 10.1201/b10163.

[51] *A Dictionary of Physics*. Oxford University Press, Jan. 2009. ISBN: 9780199233991. DOI: 10.1093/acref/9780199233991.001.0001. URL: http://www.

oxfordreference.com/view/10.1093/acref/9780199233991.001.0001/acref-9780199233991.

[52] Ray D Zimmerman and Carlos E Murillo-Sánchez. *MATP WER User's Manual Version 7.1*. Tech. rep. 2020. URL: https://matpower.org/docs/MATPOWER-manual-7.1.pdf.

[53] Qin Wang et al. "Solving corrective risk-based security-constrained optimal power flow with Lagrangian relaxation and Benders decomposition". In: *International Journal of Electrical Power & Energy Systems* 75 (Feb. 2016), pp. 255–264. ISSN: 0142-0615. DOI: 10.1016/J.IJEPES.2015.09.001.

[54] Vladan Krsman, Andrija Saric, and Neven Kovacki. "Including of branch resistances in linear power transmission distribution factors for fast contingency analysis". In: *EUROPEAN TRANSACTIONS ON ELECTRICAL POWER* 20 (2011), pp. 1–15. ISSN: 03787796. DOI: https://doi.org/10.1002/etep.618.

[55] Finn Erik Pettersen, Lars Ekern, and Vegard Willumsen. *Mapping of selected markets with Nodal pricing or similar systems. Australia, New Zealand and North American power markets*. 2011, p. 50. ISBN: 978-82-410-0742-2.

[56] Konrad Purchala et al. "Usefulness of DC power flow for active power flow analysis". In: *2005 IEEE Power Engineering Society General Meeting* 1 (2005), pp. 454–459. DOI: 10.1109/pes.2005.1489581.

A Yaml-file

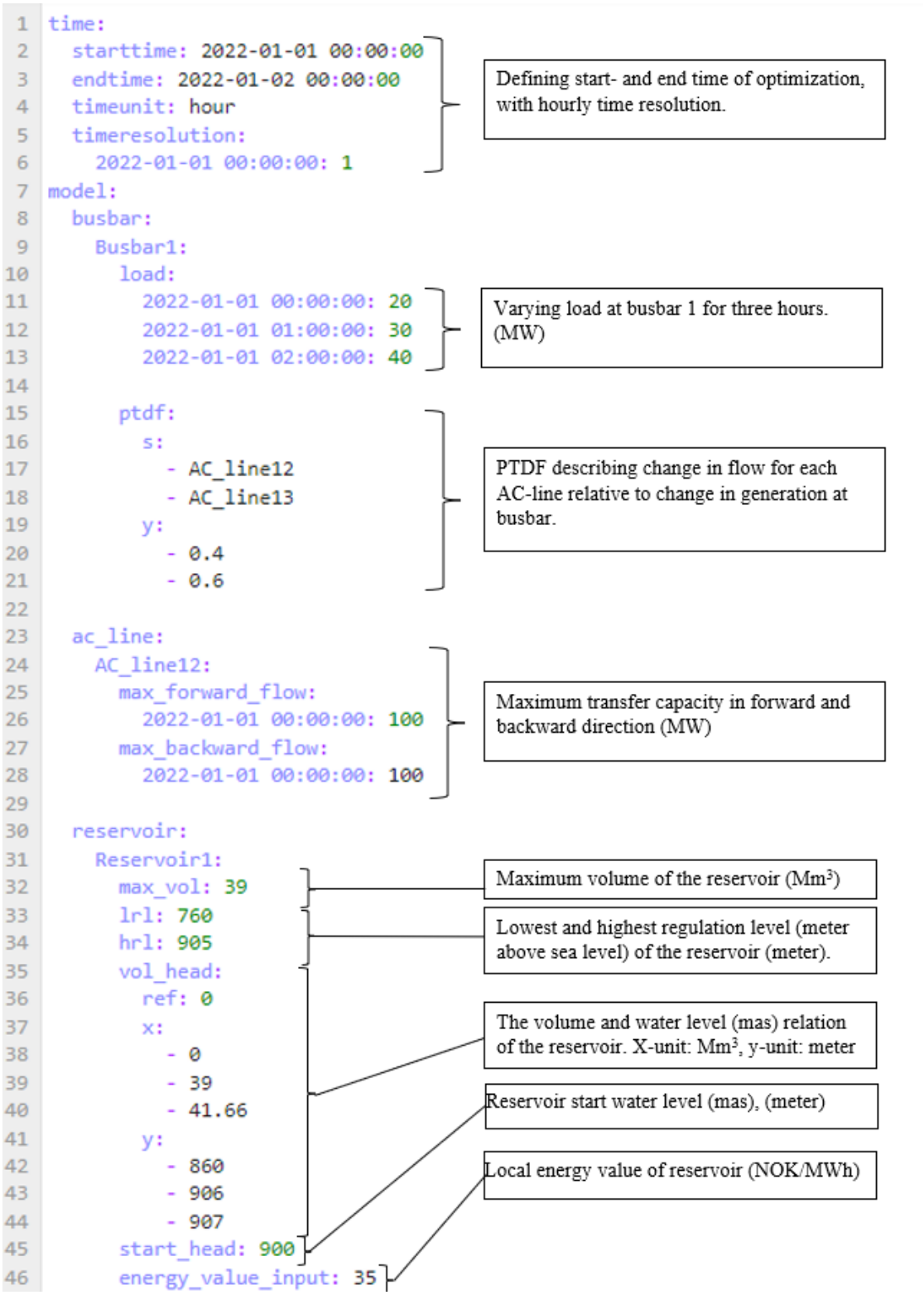

Figure A.1: *Example on input to a yaml-file. Busbar, ac-line and reservoir. The figure was constructed during the specialization project [13]. This thesis does not utilize the data provided. It is solely intended for educational purposes.*

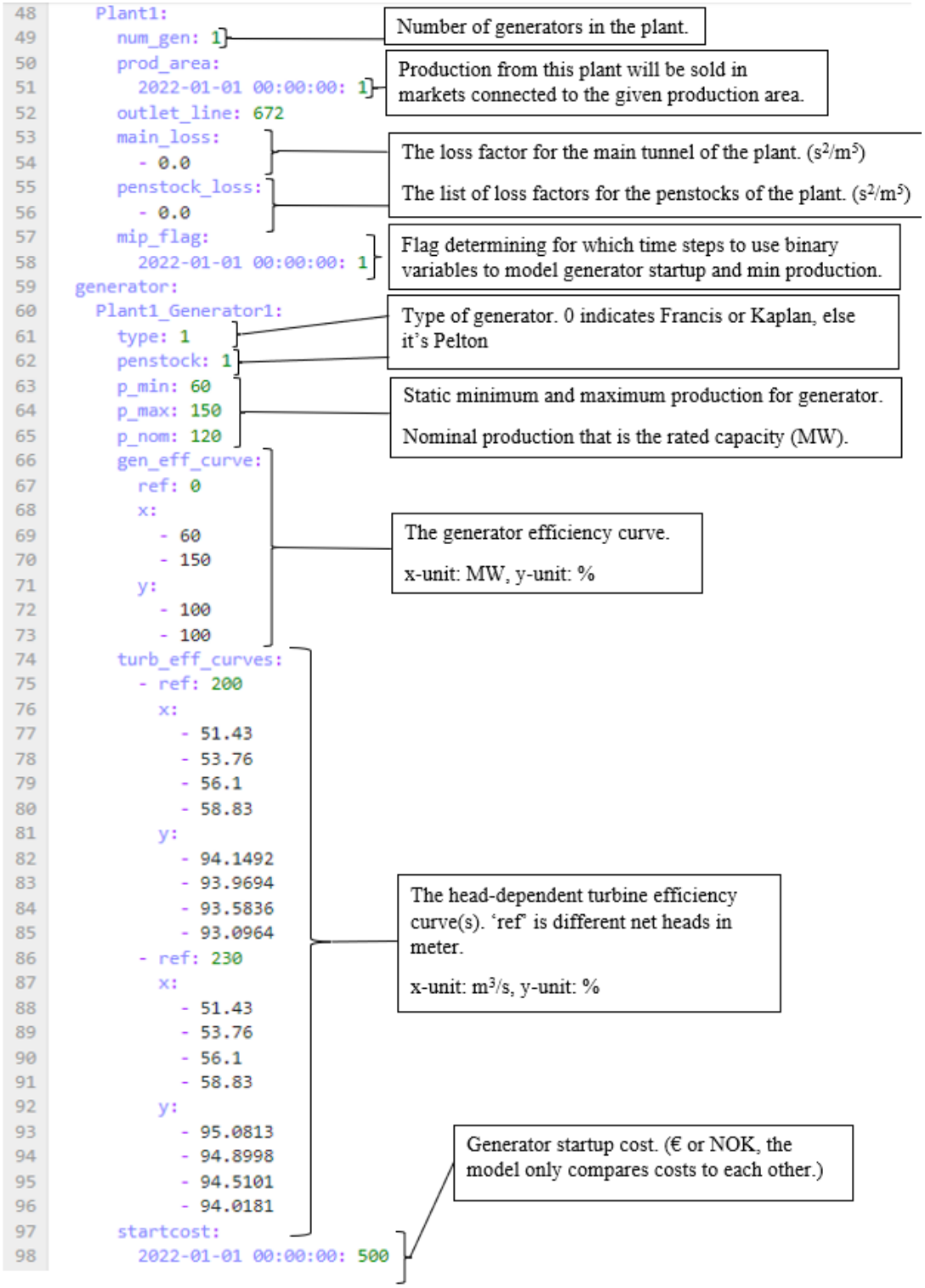

Figure A.2: *Example of input to a yaml-file. The figure was constructed during the specialization project [13].*

B Line utilization: Three cases

Table B.1: *Maximum utilization of transmission cables in three different cases for 7-day period.*

Transmission line		Utilization		
From	To	Base case	Line outage	Reduced
		Total (%)	Total (%)	Total (%)
Adamselv	Lakselv	19.2	19.2	19.2
Adamselv	Varanger (1)	11.6	11.6	11.6
Adamselv	Varanger (2)	11.6	11.6	11.6
Lakselv	Alta	17.7	18.3	17.7
Lakselv	Nedre Porsa	7.8	21.6	7.8
Alta	Alta by	25	0	25
Nedre Porsa	Alta by	10.2	18.6	10.2
Alta by	Kvænangen (1)	22	22	22
Alta by	Kvænangen (2)	33.6	33.6	33.6
Kvænangen	Nordreisa (1)	32.6	32.6	-
Kvænangen	Nordreisa (2)	24.3	24.3	-
Nordreisa	Goulasjohka (1)	29.1	29.1	-
Nordreisa	Goulasjohka (2)	16.9	16.9	-
Goulasjohka	Skibotn	13.2	13.2	-
Goulasjohka	Dividalen	6.2	6.2	-
Goulasjohka	Tromsø (1)	15.4	15.4	-
Goulasjohka	Tromsø (2)	15.4	15.4	-
Skibotn	Dividalen	8.4	8.4	-
Tromsø	Oldervik (1)	14.3	14.3	-
Tromsø	Oldervik (2)	14.3	14.3	-
Dividalen	Oldervik	12.1	12.1	-
Dividalen	Bardufoss	8.1	8.1	-
Oldervik	Bardufoss	20.5	20.5	-

C PTDF matrices

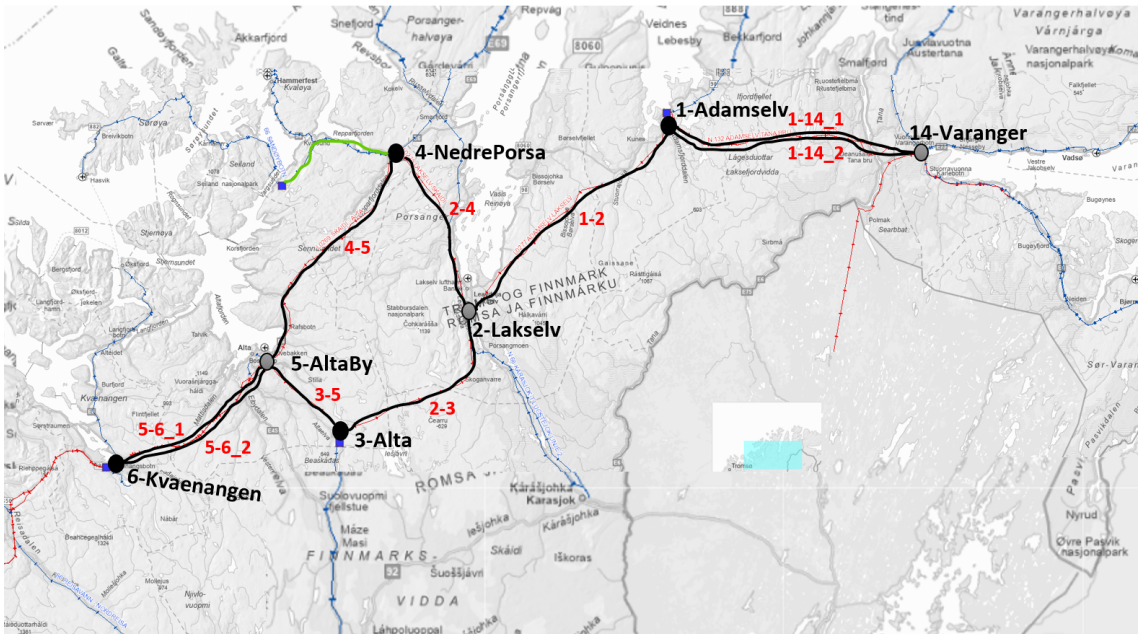

Figure C.1: *Topology of selected lines in Table C.1 for lines 2-4, 3-5 and 4-5.*

Table C.1: *PTDFs for selected lines between bus 2-4, 3-5 and 4-5. In case 2, line 3-5 is disconnected.*

Lines	2-4			3-5			4-5		
Bus	Case 1	Case 2	Case 3	Case 1	Case 2	Case 3	Case 1	Case 2	Case 3
1	0	0	0	0	-	0	0	0	0
2	0	0	0	0	-	0	0	0	0
3	-0.3189	0	-0.3189	-0.31885	-	-0.3189	-0.3189	0	-0.3189
4	-0.7303	-1	-0.7303	-0.2697	-	-0.2697	0.2697	0	0.2697
5	-0.4825	-1	-0.4825	-0.5175	-	-0.5175	-0.4825	-1	-0.4825
6	-0.4825	-1	-0.4825	-0.5175	-	-0.5175	-0.4825	-1	-0.4825
7	-0.4825	-1	-	-0.5175	-	-	-0.4825	-1	-
8	-0.4825	-1	-	-0.5175	-	-	-0.4825	-1	-
9	-0.4825	-1	-	-0.5175	-	-	-0.4825	-1	-
10	-0.4825	-1	-	-0.5175	-	-	-0.4825	-1	-
11	-0.4825	-1	-	-0.5175	-	-	-0.4825	-1	-
12	-0.4825	-1	-	-0.5175	-	-	-0.4825	-1	-
13	-0.4825	-1	-	-0.5175	-	-	-0.4825	-1	-
14	0	0	0	0	-	0	0	0	-

D Line data

Table D.1: *Line data for SHOP simulations*

AC_line	From	To	Voltage level (kV)	Present in NVE-file	Solution
1-2	Adamselv	Lakselv	132	yes	
2-3	Lakselv	Alta	132	yes	
2-4	Lakselv	NedrePorsa	132	yes	
3-5	Alta	AltaBy	132	yes	
4-5	NedrePorsa	AltaBy	132	yes	
5-6_1	AltaBy	Kvaenangen	132	yes	
5-6_2	AltaBy	Kvaenangen	132	yes	
6-7_1	Kvaenangen	Nordreisa	132	yes	
6-7_2	Kvaenangen	Nordreisa	132	yes	
7-8_1	Nordreisa	Goulasjohka	132	yes	
7-8_2	Nordreisa	Goulasjohka	132	yes	
8-9	Goulasjohka	Skibotn	132	yes	
8-10	Goulasjohka	Dividalen	420	yes	
8-11_1	Goulasjohka	Tromso	132/145	no	Estimated to have the mean reactance of two lines of similar characteristics
8-11_2	Goulasjohka	Tromso	132/145	no	Estimated to have the mean reactance of two lines of similar characteristics
9-10	Skibotn	Dividalen	132	yes	
11-12_1	Tromso	Oldervik	132/145	no	Estimated to have the mean reactance of two lines of similar characteristics
11-12_2	Tromso	Oldervik	132/145	no	Estimated to have the mean reactance of two lines of similar characteristics
10-12	Dividalen	Oldervik	132	yes	
10-13	Dividalen	BardufossResten	420	yes	
12-13	Oldervik	BardufossResten	132	yes	
1-14_1	Adamselv	Varanger	132	yes	
1-14_2	Adamselv	Varanger	132/145	no	Estimated to have the same characteristics as AC_line 1-14_1

E Water value calculation example

Below is the calculation of the water value at plant Dividalen.

1. Production data for Dividalen hydropower plant is found at NVE's hydropower database [46]. Annual energy production E_{annual} = 133.6 GWh, and rated power P_{rated} = 26 MW. Max capacity operating hours h_{max} = 133.6 GWh / 26 MW = 5138.46 h
2. Electricity price data for NO4 was downloaded from NordPool [21] with time steps of one hour (January 2022 to June 2022).
3. The price curve was sorted from high to low, and placed along an x-axis ranging from 0 to 8760.
4. Polynomial regression was performed, resulting in the curve below.

$$-2.33\cdot10^{-17}\cdot x^5+5.82\cdot10^{-13}\cdot x^4-5.57\cdot10^{-9}\cdot x^3+2.52\cdot10^{-5}\cdot x^2-5.43\cdot10^{-2}\cdot x+59.48$$

5. Using h_{max} = 5238.46 h as x in the above equation gives a water value of 13.41 €/MWh.

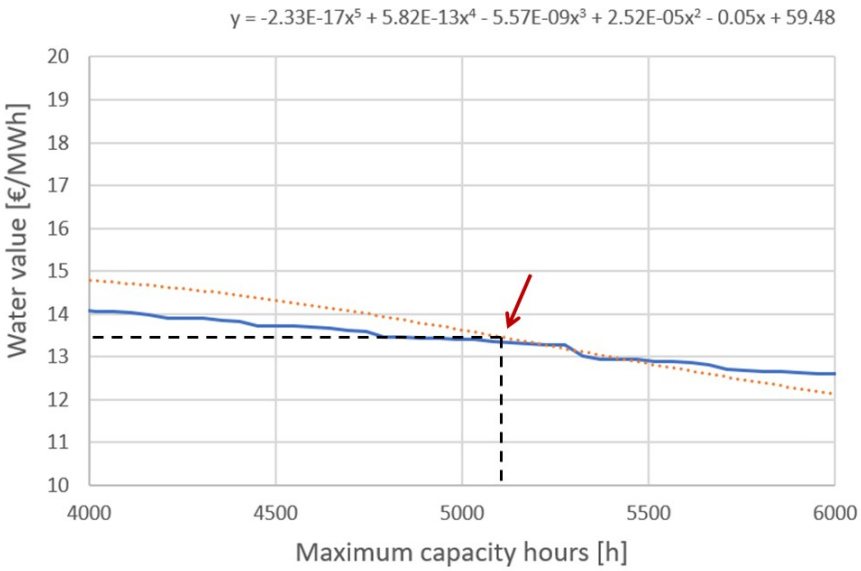

Figure E.1: *Intersection point between h_{max} = 5238.46 h and price curve.*

F Inflow calculation example

Below is the calculation of inflow at plant Dividalen.

1. Annual median inflow for Dødesvatnet (Devdisjavrri) was found on NVE atlas. The annual inflow from the precipitation field of Dødesvatnet is 160.35 $\frac{Mm^3}{year}$, which was used as Q_{normal}.
2. The nearest unregulated watercourse to Dødesvatnet was identified on NVE Sildre [48] to be Høgskarhus. For 2022, the average flow of this watercourse was 28.3 $\frac{m^3}{s}$, which results in $Q_{unregulated} = 892.4\ \frac{Mm^3}{year}$.
3. Calculated scaling factor K = $\frac{Q_{normal}}{Q_{unregulated}} = 0.18$. The scaling factor was then multiplied with the flow of Høgskarhus from 1st of January to 8th of January 2022 to get the estimated inflow of Dødesvatnet. This is shown in the Table F.1.

Table F.1: *Inflow data for Dødesvatnet and the associated unregulated watercourse Høgskarhus.*

Date	Flow Høgskarhus [m^3/s]	Inflow Dødesvatnet [m^3/s]
01.01.2022	4.51	0.81
02.01.2022	4.40	0.79
03.01.2022	4.28	0.77
04.01.2022	4.19	0.75
05.01.2022	4.07	0.73
06.01.2022	4.19	0.75
07.01.2022	4.05	0.73

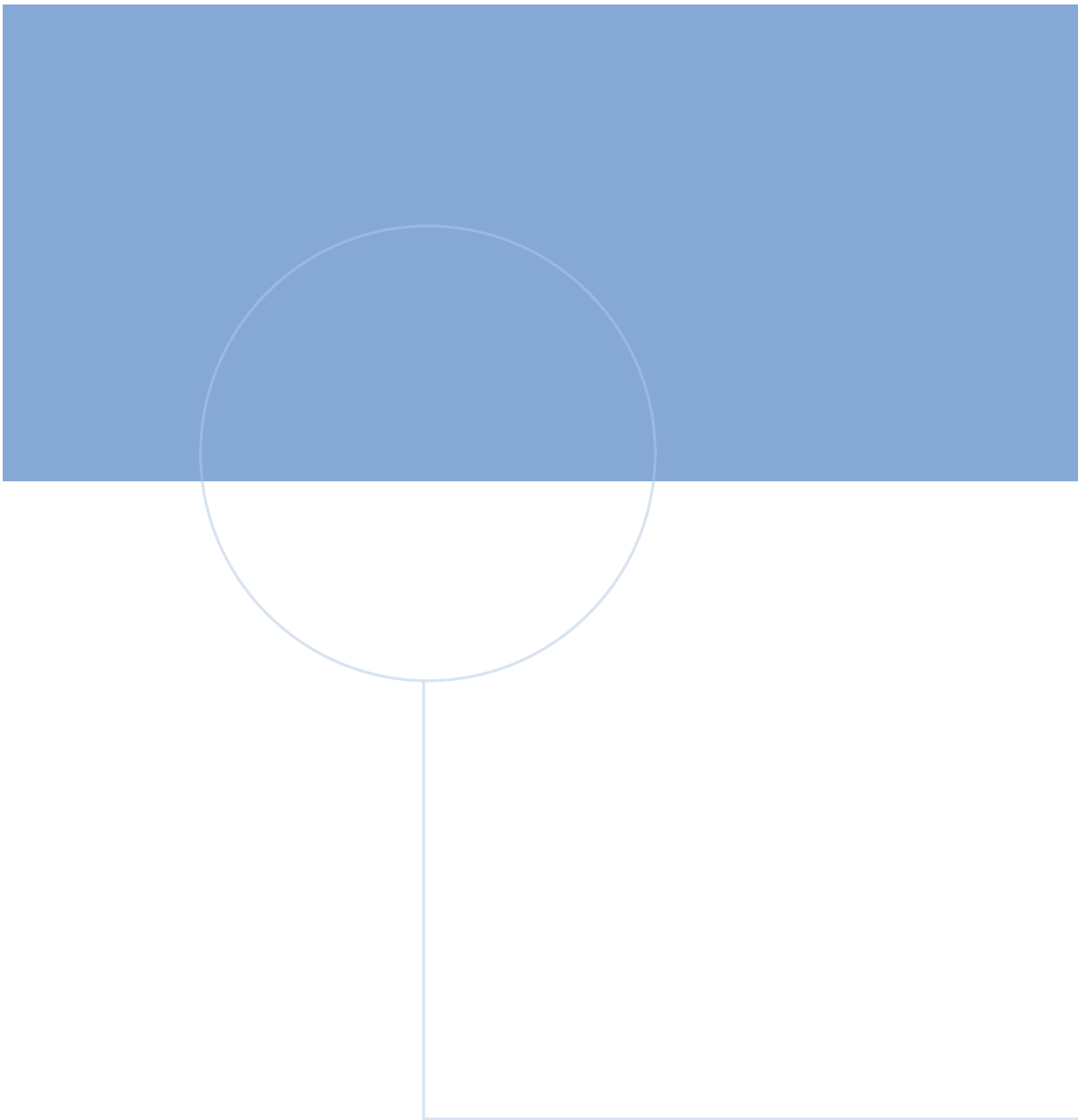

NTNU

Norwegian University of
Science and Technology